Received: 14 October 2021 | Revised: 3 April 2022 | Accepted: 15 April 2022

DOI: 10.1002/jev2.12222

RESEARCH ARTICLE

Extracellular vesicles enclosed-miR-421 suppresses air pollution ($PM_{2.5}$)-induced cardiac dysfunction via ACE2 signalling

Hongyun Wang[1,2] | **Tianhui Wang**[1,2] | **Wei Rui**[3] | **Jinxin Xie**[1,2] | **Yuling Xie**[1,2] | **Xiao Zhang**[1,2] | **Longfei Guan**[4] | **Guoping Li**[5] | **Zhiyong Lei**[6,7,8] | **Raymond M Schiffelers**[6] | **Joost P G Sluijter**[7,8] | **Junjie Xiao**[1,2]

[1]Institute of Geriatrics (Shanghai University), Affiliated Nantong Hospital of Shanghai University (The Sixth People's Hospital of Nantong), School of Medicine, Shanghai University, Nantong, China

[2]Cardiac Regeneration and Ageing Lab, Institute of Cardiovascular Sciences, Shanghai Engineering Research Center of Organ Repair, School of Life Science, Shanghai University, Shanghai, China

[3]Institute for Immunology, Tsinghua University, Beijing, China

[4]China-America Institute Neuroscience, Beijing Luhe Hospital, Capital Medical University, Beijing, China

[5]Cardiovascular Division of the Massachusetts General Hospital and Harvard Medical School, Boston, Massachusetts, USA

[6]CDL Research, University Medical Center Utrecht, Utrecht, The Netherlands

[7]Department of Cardiology, Laboratory of Experimental Cardiology, University Medical Center Utrecht, Utrecht, The Netherlands

[8]UMC Utrecht Regenerative Medicine Center, University Medical Center, Utrecht University, Utrecht, The Netherlands

Correspondence
Prof. Junjie Xiao Cardiac Regeneration and Ageing lab, Institute of Cardiovascular Sciences, Shanghai Engineering Research Center of Organ Repair, School of Life Science, Shanghai University, 333 Nan Chen Road, Shanghai 200444, China.
Email: junjiexiao@shu.edu.cn

Hongyun Wang, Tianhui Wang and Wei Rui contributed equally to this work.

Funding information
National Key Research and Development Project, Grant/Award Number: 2018YFE0113500; National Natural Science Foundation of China, Grant/Award Numbers: 82020108002, 81911540486, 82000253, 81600008; Science and Technology Commission of Shanghai Municipality, Grant/Award Numbers: 20DZ2255400, 21XD1421300; the "Dawn" Program of Shanghai Education Commission, Grant/Award Number: 19SG34; the Sailing Program from Science and Technology Commission of Shanghai, Grant/Award Number: 20YF1414000; "Chenguang Program" of Shanghai Education Development Foundation and Shanghai Municipal Education Commission, Grant/Award Number: 20CG46; Horizon2020 ERC-2016-COG EVICARE, Grant/Award Number: 725229

Abstract

Air pollution, via ambient $PM_{2.5,}$ is a big threat to public health since it associates with increased hospitalisation, incidence rate and mortality of cardiopulmonary injury. However, the potential mediators of pulmonary injury in $PM_{2.5}$-induced cardiovascular disorder are not fully understood. To investigate a potential cross talk between lung and heart upon $PM_{2.5}$ exposure, intratracheal instillation in vivo, organ culture ex vivo and human bronchial epithelial cells (Beas-2B) culture in vitro experiments were performed respectively. The exposed supernatants of Beas-2B were collected to treat primary neonatal rat cardiomyocytes (NRCMs). Upon intratracheal instillation, subacute $PM_{2.5}$ exposure caused cardiac dysfunction, which was time-dependent secondary to lung injury in mice, thereby demonstrating a cross-talk between lungs and heart potentially mediated via small extracellular vesicles (sEV). We isolated sEV from $PM_{2.5}$-exposed mice serum and Beas-2B supernatants to analyse the change of sEV subpopulations in response to $PM_{2.5}$. Single particle interferometric reflectance imaging sensing analysis (SP-IRIS) demonstrated that $PM_{2.5}$ increased CD63/CD81/CD9 positive particles. Our results indicated that respiratory system-derived sEV containing miR-421 contributed to cardiac dysfunction post-$PM_{2.5}$ exposure. Inhibition of miR-421 by AAV9-miR421-sponge could significantly reverse $PM_{2.5}$-induced cardiac dysfunction in mice. We identified that cardiac angiotensin converting enzyme 2 (ACE2) was a downstream target of sEV-miR421, and induced myocardial cell apoptosis and cardiac dysfunction. In addition, we observed that GW4869 (an inhibitor of sEV release) or diminazene aceturate (DIZE, an activator of ACE2) treatment could attenuate $PM_{2.5}$-induced cardiac

dysfunction in vivo. Taken together, our results suggest that $PM_{2.5}$ exposure promotes sEV-linked miR421 release after lung injury and hereby contributes to $PM_{2.5}$-induced cardiac dysfunction via suppressing ACE2.

KEYWORDS
PM2.5, cardiac dysfunction, extracellular vesicles, miR-421, ACE2

1 | INTRODUCTION

Ambient fine particulate matter ($PM_{2.5}$, aerodynamic diametre $\leq 2.5\mu$m) became a leading cause of air pollution in the past few years. With the improvement of air quality, the continuous pollution weather gradually decreases, although the sudden acute pollution occurs in northern China in winter (Li et al., 2021; Zhang et al., 2019). Few studies have examined, however, the effect and biological mechanism of $PM_{2.5}$ exposure upon relatively short-term pollution. The damage of short-term $PM_{2.5}$-exposure to human body should not be ignored. Increasing evidence demonstrated that acute or subacute $PM_{2.5}$ exposure could increase the hospitalisation rate and mortality of all related diseases (Atkinson et al., 2014), especially cardiovascular diseases (CVD) (Dominici et al., 2006). In short term, the increase of atmosphere $PM_{2.5}$ concentration is positively correlated with total mortality, especially cardiovascular and respiratory disease mortality (Liu et al., 2019). In addition, animal experiments showed that short-term and subacute $PM_{2.5}$ exposure leads to cardiac dysfunction, including myocardial cells apoptosis (Gao et al., 2020) and right ventricular hypertrophy (Yue et al., 2019), etc. However, the molecular mechanism of cardiac dysfunction induced by subacute respiratory exposure to $PM_{2.5}$ is not fully clear. Moreover, the effect of pulmonary injury on $PM_{2.5}$-induced cardiac dysfunction is not understood.

Pulmonary disease or subclinical pulmonary dysfunction can affect cardiovascular function and are linked to the increased risk of CVD such as hypertension (Jacobs et al., 2012) and atherosclerosis (Barr et al., 2012). It was found that respiratory tract exposure to cigarette smoke and pollutants can cause cardiac dysfunction (Van Eeden et al., 2012), which is mainly associated with blood oxygen deficiency, hypercapnia and intrathoracic pressure changes. A direct correlation between cardiac dysfunction and lung injury exists (Barnes et al., 2015; Nishiyama et al., 2010), which may contribute to cardiac injury after exposure to air pollution. The biological basis of the dialogue between lungs and heart contains three aspects, namely interconnection via gas exchange, body fluids and mechanical interaction. However, $PM_{2.5}$-tracing has not been solved, and there is no evidence demonstrating that $PM_{2.5}$ can deposit directly in blood vessels. Therefore, the above mechanism cannot fully answer the mechanism of $PM_{2.5}$ induced cardiovascular injury, and the molecular mechanism of $PM_{2.5}$ induced myocardial injury and cardiac dysfunction warrants further study.

Interestingly, a previous study demonstrates that short-term particulate matter exposure-induced increase coagulation is associated with extracellular vesicle-packaged miRNA release (Pergoli et al., 2017), which suggests extracellular vesicles (EVs) are involved in PM-induced dysfunction. In addition, another study shows that glutaminase-containing EVs may serve as a potential mediator in $PM_{2.5}$-induced neurotoxicity (Chen et al., 2020).

Small extracellular vesicles (sEV) are membrane enclosed nanoparticles, with a diametre of 40–200 nm, which can be released by almost all kinds of cells and exist in multiple biofluids such as milk, urine, and saliva (Sluijter et al., 2018; Wang et al., 2020). Increasing evidence demonstrates that EVs can delivery biological molecules including microRNAs (miRNAs, miRs), proteins and lipids and facilitate intercellular communication, taking important roles in multiple physiological and pathological processes (Femminò et al., 2020; Kalluri & Lebleu, 2020; O'brien et al., 2020). However, the changes of extracellular subpopulations in response to $PM_{2.5}$ exposure as well as the role of sEV in respiratory $PM_{2.5}$ exposure-induced cardiac dysfunction remains to be elucidated. The mechanism of crosstalk between lungs and heart, mediated by sEV in response to $PM_{2.5}$ is still not clearly. In the present study, we utilised a subacute exposure model in vivo (by intratracheal instillation) and an acute model in vitro to evaluate the role of respiratory system-released sEV in $PM_{2.5}$ exposure-induced cardiac dysfunction. We also explored the mechanism of sEV mediated crosstalk between lungs and heart in response to $PM_{2.5}$ exposure.

2 | MATERIALS AND METHODS

2.1 | $PM_{2.5}$ collecting and analysis

$PM_{2.5}$ particle used in the present study were collected at Tsinghua University, whose characterisation is similar to our previous study (Wang et al., 2018). Briefly, $PM_{2.5}$ were continuously collected using a sampler particle collector with a flux of 115 L/min and thermo high flow sampler (1 m^3/min). During this process, Teflon membranes (with a diametre of 90 mm) were used to collect

particles. The collected $PM_{2.5}$ were sterilised by Co-60 irradiation, and dissolved in deionised water, and vortexed for 0.5 min prior to use.

2.2 | Animal experiments

Wild-type C57BL/6 J male mice, 8-week-old, were purchased from Charles River labs (Beijing, China) and used for animal experiments. All animal experiments in the present study were approved by the Ethics Committee of Shanghai University (approval number: 2020-037).

To establish this subacute $PM_{2.5}$ exposure model, mice received 2.5–3.6 mg/kg $PM_{2.5}$ in 10 μl phosphate buffer saline (PBS) via intratracheal instillation for 14 consecutive days (the first exposure day was labelled as day1 and the last exposure day was labelled as day14), followed by echocardiography measurement at day15, day21, day28 and day35. Notably, there is no $PM_{2.5}$ exposure from day15 to day35. Echocardiographic images were obtained with a Visualsonics high-resolution Veve 2100 system as previously described (Wang et al., 2018). All mice were sacrificed at day36 and the lung and heart tissues were harvested.

Eight-week-old wild-type mice received intraperitoneal injections of an inhibitor of extracellular vesicles (GW4869, 2.5 mg/kg) or dimethyl sulfoxide (DMSO) every 48 h (Xu et al., 2020) till day35. In addition, to investigate the effect of miR-421 knockdown in $PM_{2.5}$-induced cardiac dysfunction, we constructed adeno-associated virus 9 (AAV9)-miR421-sponge to knock down mmu-miR421 in mice. Briefly, mice received AAV9-miR421-sponge and its control at a dose of 10^{12}vg/mice via tail vein injection 1 day before $PM_{2.5}$ instillation. As mentioned above, the mice received echocardiography measurement at day35 and sacrificed at day36. The lungs and heart tissue were harvested. As described privously (Evans et al., 2020), the mice received daily intraperitoneal injections of Diminazene aceturate (DIZE, 15 mg/kg per day) or saline treatment for 30 days.

2.3 | Cell culture and treatment

2.3.1 | Beas-2B

As previously described (Wang et al., 2018), the human bronchial epithelial cell line Beas-2B was maintained in Dulbecco's modified Eagle medium (DMEM) supplemented with 10% fetal bovine serum (FBS) and 1% penicillin and streptomycin (PS). After culture overnight, the cells were transfected by miR-421 inhibitor (purchased from Guangzhou RiboBio Co., Ltd. China) for 48 h followed by $PM_{2.5}$ exposure for 24 h ($PM_{2.5}$ were diluted in DMEM to final concentration of 50 μg/ml and equal volume of PBS in DMEM was control). The culture medium was then collected and centrifugated at 3000 × *g* for 5 min at 4°C to obtain the supernatants of PBS or $PM_{2.5}$ exposed Beas-2B (labelled as SB-Ctr and SB-$PM_{2.5}$, respectively), which can be used immediately or stored at −20°C for use. For sEV blockade, the cells were pretreated with GW4869 (20 μM) for 12 h prior to $PM_{2.5}$ exposure.

2.3.2 | Neonatal rat cardiomyocytes (NRCMs)

Primary NRCMs were separated from neonatal rats as described previously (Bei et al., 2017). To investigate cell to cell crosstalk between lungs and heart, mice serum-derived sEV, ex vivo fluids (Ex-Ctr or Ex-$PM_{2.5}$) and cell supernatants of Beas-2B (SB-Ctr or SB-$PM_{2.5}$) were obtained respectively (Figure 1a). NRCMs were transfected by overexpressed human (h)-ACE2/vehicle plasmid or ACE2-siRNA/scramble siRNA for 48 h followed by 24 h exposure to sEV, ex vivo fluids, and cell supernatants of Beas-2B. For DIZE treatment, NRCMs were isolated and pretreated with 100 nm of DIZE for 48 h prior to SB-$PM_{2.5}$ or SB-Ctr exposure. To verify the role of inducible nitric oxide synthase (iNOS) in $PM_{2.5}$-induced cardiomyocytes, 500 μM of NG-Nitro-L-arginine Methyl Ester, Hydrochloride (L-NAME) was used to treat NRCMs for 30 min followed by SB-Ctr or SB-$PM_{2.5}$ exposure for 24 h.

2.3.3 | Human umbilical vein endothelial cells (HUVEC)

HUVEC was maintained in DMEM supplemented with 10% FBS and 1% PS. To assess the effect of $PM_{2.5}$ on endothelial injury, HUVEC was cultured overnight followed by SB-Ctr or SB-$PM_{2.5}$ exposure for 24 h and endothelial NOS (eNOS)/iNOS were examined.

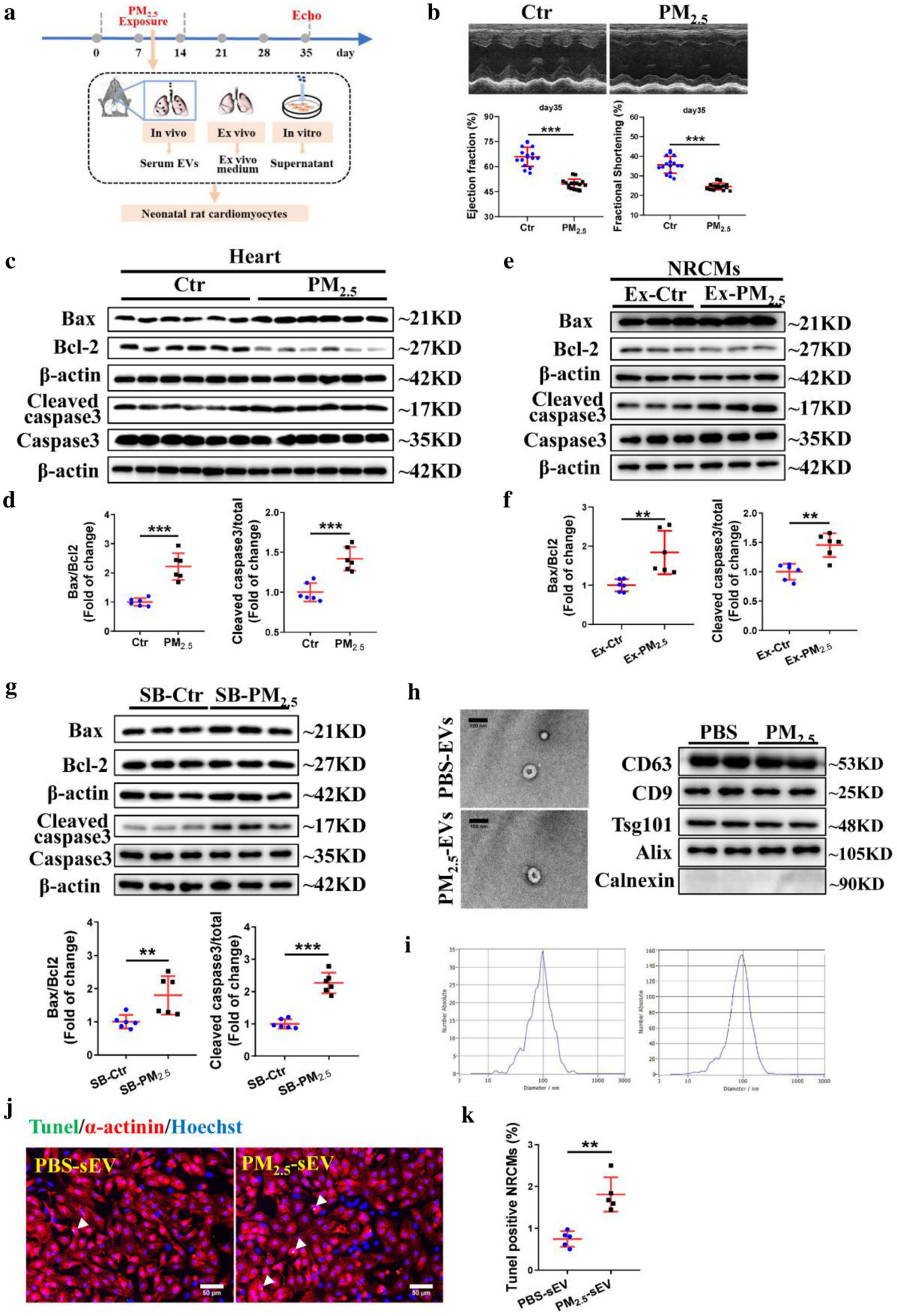
a
PM2.5 Exposure
Echo
0 7 14 21 28 35 day
In vivo
Ex vivo
In vitro
Serum EVs
Ex vivo medium
Supernatant
Neonatal rat cardiomyocytes
b
Ctr
PM2.5
day35
Ejection fraction (%)
Fractional Shortening (%)
***
c
Heart
Ctr
PM2.5
Bax
Bcl-2
β-actin
Cleaved caspase3
Caspase3
β-actin
~21KD
~27KD
~42KD
~17KD
~35KD
~42KD
e
NRCMs
Ex-Ctr
Ex-PM2.5
d
Bax/Bcl2 (Fold of change)
Cleaved caspase3/total (Fold of change)
f
**
g
SB-Ctr
SB-PM2.5
h
PBS-EVs
PM2.5-EVs
PBS
PM2.5
CD63
CD9
Tsg101
Alix
Calnexin
~53KD
~25KD
~48KD
~105KD
~90KD
i
Number Absolute
Diameter / nm
j
Tunel/α-actinin/Hoechst
PBS-sEV
PM2.5-sEV
k
Tunel positive NRCMs (%)

2.4 | Ex vivo organ culture

After GW4869 injection and $PM_{2.5}$ exposure, mice lung and bronchi were dissected and segmented into pieces. These segments were cultured in DMEM (with 1% penicillin/streptomycin) and incubated at 95% carbon dioxide, 37°C overnight (Manson et al., 2020). Then, the segments were transferred to fresh medium and the ex vivo culture supernatants were collected after 48 h, stored at −20°C for use.

2.5 | Isolation of sEV from mice serum and cell supernatants

The blood was collected and then clotted for 30 min at room temperature. Centrifuging the serum at 10,000 × *g* for 10 min at 4°C to remove any remaining insoluble material as described previously (Greenfield, 2017). The serum was immediately used for sEV isolation.

To isolate sEV from mice serum, size exclusion chromatography (SEC) was used. Briefly, 500 μl pooled serum from three independent mice were loaded in qEV original columns (35 nm, SP5102099, Izon), obtaining 1.5 ml per fraction. The fraction was concentrated by Amicon Ultra-4 10KD centrifugal filters (Merck Millipore, #UFC801096) for 50 min at 4000 rpm.

For isolating sEV from Beas-2B cell supernatants, differential ultracentrifugation was used. Total 10 ml of cell supernatants/sample underwent serial centrifugated at 500 × *g* for 10 min, 3000 for 10 min, 12,000 × *g* for 45 min and 100,000 × *g* for 70 min. The sEV pallets were suspended by 100 μl PBS for immediately use.

2.6 | Characterisation of EVs

For morphological observation, 10 μl of fresh sEV were prepared for Transmission electron microscope (TEM) imaging. The TEM image was obtained using FEI Tecnai G2 F20 TEM (USA).

For size and concentration analysis, sEV was diluted in filtered PBS and examined by Zetaview (Particle Metrix, Germany). For each sample, three cycles were performed (11 positions for each) under following settings: min brightness: 20, Max size:1000, Min size:5, Sensitivity: 70.0, Frame rate: 30 and shutter: 70.

Protein markers of EVs (CD9, CD63, Tsg101) and negative marker (calnexin) were examined by western blotting. Briefly, sEV was lysed with EV-specific lysis buffer (Umibio, #UR33101, Shanghai, China) as described previously (Zhou et al., 2021). Bicinchoninic acid protein assay kit was used to assess the protein concentration of sEV and 10 μg of protein were used to perform western blotting.

2.7 | Single particle interferometric reflectance imaging sensing analysis (SP-IRIS)

SP-IRIS measurement was performed as previously described (Arab et al., 2021). The EVs, derived from three independent samples, were pooled and then divided into three pieces for subsequent analysis. Briefly, diluting 35 μl of EVs in incubation buffer (IB) (1:1) and incubating them on ExoView R100 (NanoView Biosciences, Brighton, MA) chips at room temperature for 16 h. Notably, the chips were coated with antibodies against antihuman CD81, CD63 and CD9 respectively. Anti-mouse IgG was used as negative control. Then, washing the chips with IB for 3 min × 4 at 500prm and incubated for next 1 h with fluorescent

FIGURE 1 Cardiac dysfunction is secondary to lung injury and crosstalk occurred after $PM_{2.5}$ exposure in vivo. (a) Schematic representation of experimental design in vivo, ex vivo and in vitro. To make subacute $PM_{2.5}$ exposure model, mice received $PM_{2.5}$ or PBS exposure via intratracheal instillation every day for 2 weeks (the first exposure day was labelled as day1 and the last exposure day was labelled as day14), followed by echocardiography measurement at day15, day21, day28 and day35, respectively. For ex vivo culture, the PBS or $PM_{2.5}$ exposed mice lung and bronchi were dissected and the segments were cultured for 48 h. We then collected the ex vivo culture supernatants for use. For in vitro culture, the human bronchial epithelial cell line Beas-2B exposed to $PM_{2.5}$ for 48 h and collected the supernatants for centrifugation. Then the supernatants were collected for use. These supernatants were used to treat primary neonatal rat cardiomyocytes for 24 h. (b) Qualification of cardiac ejection fraction (EF) and fraction shorting (FS) at day35 in mice. $n = 16$. (c) Representative images obtained by western blot to show the protein expression of Bax, Bcl-2, cleaved caspase 3 and caspase 3 in heart tissues lysates of mice. (d) Qualification of the ratio of Bax/Bcl-2 and cleaved caspase 3/total caspase 3. $n = 6$. (e) Western blot images of Bax, Bcl-2, cleaved caspase 3 and caspase 3 and (f) quantitation results of these proteins in Ex-Ctr and Ex-$PM_{2.5}$ exposed NRCMs. $n = 6$. (g) Protein expression of Bax, Bcl-2, cleaved caspase 3 and caspase 3 in SB-Ctr or SB-$PM_{2.5}$ exposed NRCMs, $n = 6$. (h) TEM images and marker proteins of mice serum-derived sEV. Scale bar = 100 nm (i) Concentration and size of serum-derived sEV were tested by nanoparticle tracking analysis (Zetaview). (j) Representative images of TUNEL/α-actinin/Hoechst staining of PBS-sEV or $PM_{2.5}$-sEV exposed NRCMs. Scale bar = 50μm. (k) Quantitation of TUNEL positive NRCMs after PBS-sEV or $PM_{2.5}$-sEV treatment. $n = 5$. Data were represented as mean ± SD. $^{**}p < 0.01$ and $^{***}p < 0.001$, from comparing PBS- and $PM_{2.5}$-exposed groups, calculated by unpaired Student's t-test (two-sided). ***Ex-Ctr***: ex-vivo culture supernatants of PBS-exposed mice lung and bronchi. ***Ex-PM$_{2.5}$***: ex vivo culture supernatants of $PM_{2.5}$-exposed mice lung and bronchi. ***SB-Ctr***: Supernatants of PBS-exposed Beas-2B cells. ***SB-PM$_{2.5}$***: Supernatants of $PM_{2.5}$-exposed Beas-2B cells. ***PBS-sEV***: Small EVs derived from PBS-exposed mice serum. ***PM$_{2.5}$-sEV***: Small EVs derived from $PM_{2.5}$-exposed mice serum

antibodies against CD81, CD63 and CD9 (1:1200) in blocking buffer (1:1 mixture of IB and blocking buffer). Subsequently, the chips underwent washing with IB, wash buffer and rinse buffer and then immersed in rinse buffer for 5 s. After fully dry, the chips were imaged by ExoView scanner (NanoView Biosciences, Brighton, MA). Finally, all data were analysed using NanoViewer 2.8.10 Software (NanoView Biosciences).

2.8 | TUNEL staining

Mice lung and heart tissues were harvested and fixed with 4% paraformaldehyde fix solution (PFA) for 48 h and embedded in paraffin. Paraffin section of heart and lung (5 μm) were stained by TUNEL kit (A112-01/02/03, Vazyme, China) and followed by α-actinin/Hoechst staining to assess cell apoptosis according to the manufacturer's instructions. Immediately, immunofluorescence staining with α-actinin antibody were performed to label cardiomyocytes. To assess NRCMs apoptosis in vitro, NRCMs were fixed in 4% PFA for 20 min at room temperature and then incubated with 0.5% Triton X-100, followed by α-actinin immunostaining overnight and TUNEL/Hoechst staining.

2.9 | Plasmid and siRNA information

In the present study, micrOFF mmu-miR-421-3p inhibitor, ACE2 siRNA and negative control were purchased from RiboBio Co., LTD (Guangzhou, China). Human-ACE2 overexpressed plasmid (pLENTI_hACE2_PURO) was a gift from Raffaele De Francesco (Addgene plasmid #155295; http://n2t.net/addgene:155295; RRID: Addgene_155295). The empty backbone (pLenti-puro) was a gift from Ie-Ming Shih (Addgene plasmid #39481; http://n2t.net/addgene:39481; RRID: Addgene_39481) (Guan et al., 2011). The AAV system comprised of pAAV-MCS, AAV2/9 and deltaF6. Mouse miR-421-3p sponge (target sequence: 5′-GCGCCCAATTAATAGAGTTGAT-3′) and scramble control were cloned as previous described (Kimura et al., 2019).

2.10 | Statistical analysis

The data were reported as means ± standard deviation (SD) with the sample size. All statistical analysis were conducted using GraphPad Prism 8 software. All the sample sizes (n) were shown in figure legends. *p*-value were determined by unpaired Student's *t* test (two sided) as well as one or two-way ANOVA with Tukey correction for comparisons between different groups when the normality test is passed and variances are equal. Nonparametric analysis was used when variances were significantly different or non-normal distribution. A p-values<0.05 were considered as statistically significant.

3 | RESULTS

3.1 | Subacute respiratory system exposure to $PM_{2.5}$ causes lung injury

To investigate the effect of subacute $PM_{2.5}$ exposure on cardiac function, mice received $PM_{2.5}$ via intratracheal instillation every day for 14 days. Cell number and protein concentration in bronchoalveolar lavage fluid (BALF) and pulmonary TNF-α levels were assayed to assess pulmonary inflammatory reaction after $PM_{2.5}$ exposure. Intratracheal inhalation of $PM_{2.5}$ for 14 days causes a robust increase in cell number and protein concentration of BALF (Figure S1A and S1B), as well as TNF-α level (Figure S1C) in lungs, demonstrating an inflammatory reaction that occurred in the lungs after subacute $PM_{2.5}$ exposure. We assessed reduced/oxidised glutathione (GSH and GSSG) in lungs to assess oxidative stress in response to $PM_{2.5}$. After $PM_{2.5}$ exposure, the ratio of GSH/GSSG in lungs was reduced in $PM_{2.5}$-exposed lungs compared to that of control (Figure S1D). We then performed hematoxylin-eosin (H&E) staining, TUNEL staining and apoptotic protein analysis in exposed lungs. The diametre of collapsed alveoli increased ~2 folds after $PM_{2.5}$ exposure (Figure S1E). TUNEL positive cells (Figure S1F) and relative Bax/Bcl-2, cleaved caspase3/total caspase3 (Figure S1G) significantly increased after $PM_{2.5}$ exposure. All these data demonstrated that subacute $PM_{2.5}$ exposure via respiratory system caused lung inflammation, oxidative stress and an induction of local cell apoptosis.

3.2 | Cardiac dysfunction is secondary to lung injury after exposure to $PM_{2.5}$ in vivo

To confirm a subsequent cross talk between lung and heart induced by $PM_{2.5}$, we designed experiments in vivo, ex vivo and in vitro, respectively (details depicted in Figure 1a). After 14-day of $PM_{2.5}$ exposure, serial echocardiography measurement at day15, day21, day28 and day35 were performed to assess cardiac function in mice. The $PM_{2.5}$-exposed mice exhibited a significant lower

ejection fraction (EF) and fractional shortening (FS) than that of controls, which was pronounced between $PM_{2.5}$ and control group at day35 (Figure 1b). As clearly visible in time, cardiac systolic function was gradually reduced in the $PM_{2.5}$-exposed mice (Figure S1H), which suggest prolonged time-effects after $PM_{2.5}$ exposure.

To further investigate the potential effect of $PM_{2.5}$-induced lung injury on the heart, cardiac apoptosis protein markers were assessed at day36. As shown in Figure 1c and d, respiratory exposure to $PM_{2.5}$ significantly increased the ratio of Bax/Bcl-2, and cleaved caspase 3/total caspase 3 in mice heart (Figure 1c and d).

To evaluate whether cardiac dysfunction is related to $PM_{2.5}$-induced lung injury, we isolated $PM_{2.5}$- or PBS-exposed lung and bronchi to culture ex vivo and collected these exposed ex vivo fluids to treat NRCMs subsequently. The $PM_{2.5}$-exposed ex-vivo fluids (Ex-$PM_{2.5}$) contribute to an elevated Bax/Bcl-2 and cleaved caspase3/total caspase3 in NRCMs compared to Ex-Ctr exposed group. (Figure 1e and f).

Epithelial cells are important for respiratory function in lungs and several chronic pulmonary diseases have a common pathobiology basis of epithelial repair dysfunction (Guillot et al., 2013; Spella et al., 2017). To investigate whether post $PM_{2.5}$-exposure induced cardiac dysfunction is associated with epithelial cells, we utilised human bronchial epithelial cells (Beas-2B) and exposed them to $PM_{2.5}$ in vitro and collected the supernatant followed by centrifugation at 3000 × *g* for 5 min. Subsequently, we exposed NRCMs with the supernatants of $PM_{2.5}$ or PBS exposed Beas-2B cells for 24 h and assessed cell apoptosis (labelled with SB-$PM_{2.5}$ and SB-Ctr, respectively). SB-$PM_{2.5}$ exposure caused increases in Bax/Bcl-2 and cleaved caspase3/total caspase3 compared to SB-Ctr (Figure 1g). All these data demonstrated that subacute $PM_{2.5}$-exposure induced cardiac dysfunction could be mediated via a damage to lung epithelium.

During long-term $PM_{2.5}$ exposure, oxidative and inflammatory reaction were identified as mediators of cardiac dysfunction or cardiomyocytes apoptosis (Newby et al., 2015; Pope et al., 2016). To investigate whether inflammatory mediators affected cardiac function in our model, inflammatory factors (TNFα, IL-1β, IL-6) were assessed in mice at day36. Within the respiratory system, short-term exposure of $PM_{2.5}$ slightly but not significantly changed cardiac inflammatory factors (Figure S2A), suggesting an inflammatory-independent pathway occurred in $PM_{2.5}$-induced cardiac dysfunction.

To further investigate the potential cross talk between lungs and heart, we separated sEV from mice serum and used these sEV to evaluate the effect of lung injury on cardiomyocytes apoptosis in vitro. sEV characterisation demonstrated a typical cup-shaped structure (Figure 1h), with an average diametre of 95 ± 5 nm in both groups (Figure 1i). The presence of typical protein markers such as CD9, CD63, Tsg101, Alix and negative marker (calnexin) were shown in Figure 1h. Approximately 40 μg of total sEV protein was supplemented to the FBS-free culture medium of NRCMs for 48 h. NRCMs were subjected to TUNEL staining after sEV treatment. $PM_{2.5}$-sEV exposure significantly increased the number of TUNEL positive cardiomyocytes compared to PBS-sEV (Figure 1j and k), indicating $PM_{2.5}$-sEV exacerbated NRCMs apoptosis.

Together, these results demonstrated that subacute $PM_{2.5}$ exposure induced cardiac dysfunction was connected to lung injury, which is time dependent. Moreover, a potential crosstalk mediated by EVs may exist between lungs and heart in response to $PM_{2.5}$ exposure.

3.3 | $PM_{2.5}$ exposure promotes EVs secretion via altering extracellular subpopulations

We speculated that EVs may be involved in the crosstalk between lungs and heart upon $PM_{2.5}$ exposure. To confirm this hypothesis, we isolated EVs from $PM_{2.5}$-exposed Beas-2B supernatants and measured these EVs through SP-IRIS. The enriched EVs, SB-Ctr-EVs and SB-$PM_{2.5}$-EVs, both displayed a cup-shaped morphology by TEM (Figure 2a). Interestingly, SP-IRIS analysis indicated that $PM_{2.5}$ exposure promotes EVs secretion via increasing the number of CD63-positive, CD-81 positive and CD-9 positive EVs compared to control group (Figure 2b). Protein markers such as CD63, CD9, Tsg101, Alix and negative marker Calnexin were shown by western blot (Figure 2c). Similar size (60 ± 4 nm) of SB-Ctr-EVs and SB-$PM_{2.5}$-EVs were displayed by SP-IRIS (Figure 2d). Immuno-colocalisation imaging indicated that $PM_{2.5}$ exposure did increase the number of CD63/CD81/CD9 colocalisation EVs compared to control group (Figure 2e). These data demonstrated that $PM_{2.5}$ exposure significantly increased CD63, CD81 and CD9 positive nanoparticles in vitro.

3.4 | GW4869 improves sub-acute $PM_{2.5}$-induced cardiac dysfunction in vivo

To validate whether small EVs mediated $PM_{2.5}$-induced cross talk between lungs and heart, GW4869, an inhibitor of sEV release, was used. GW4869 injection significantly reversed $PM_{2.5}$-induced EF and FS reduction (Figure 3a and b), demonstrating that inhibition of sEV attenuates $PM_{2.5}$-induced cardiac dysfunction. Mice heart slices were used for TUNEL staining/α-actinin immunostaining/Hoechst staining to evaluate cardiomyocytes apoptosis in $PM_{2.5}$-exposed mice. Post-$PM_{2.5}$ exposure caused an increase in TUNEL positive cardiomyocytes in the slices and GW4869 injection significantly reversed $PM_{2.5}$-induced cardiomyocytes apoptosis (Figure 3c). Western blotting results indicated that subacute $PM_{2.5}$ exposure caused cardiac apoptosis via

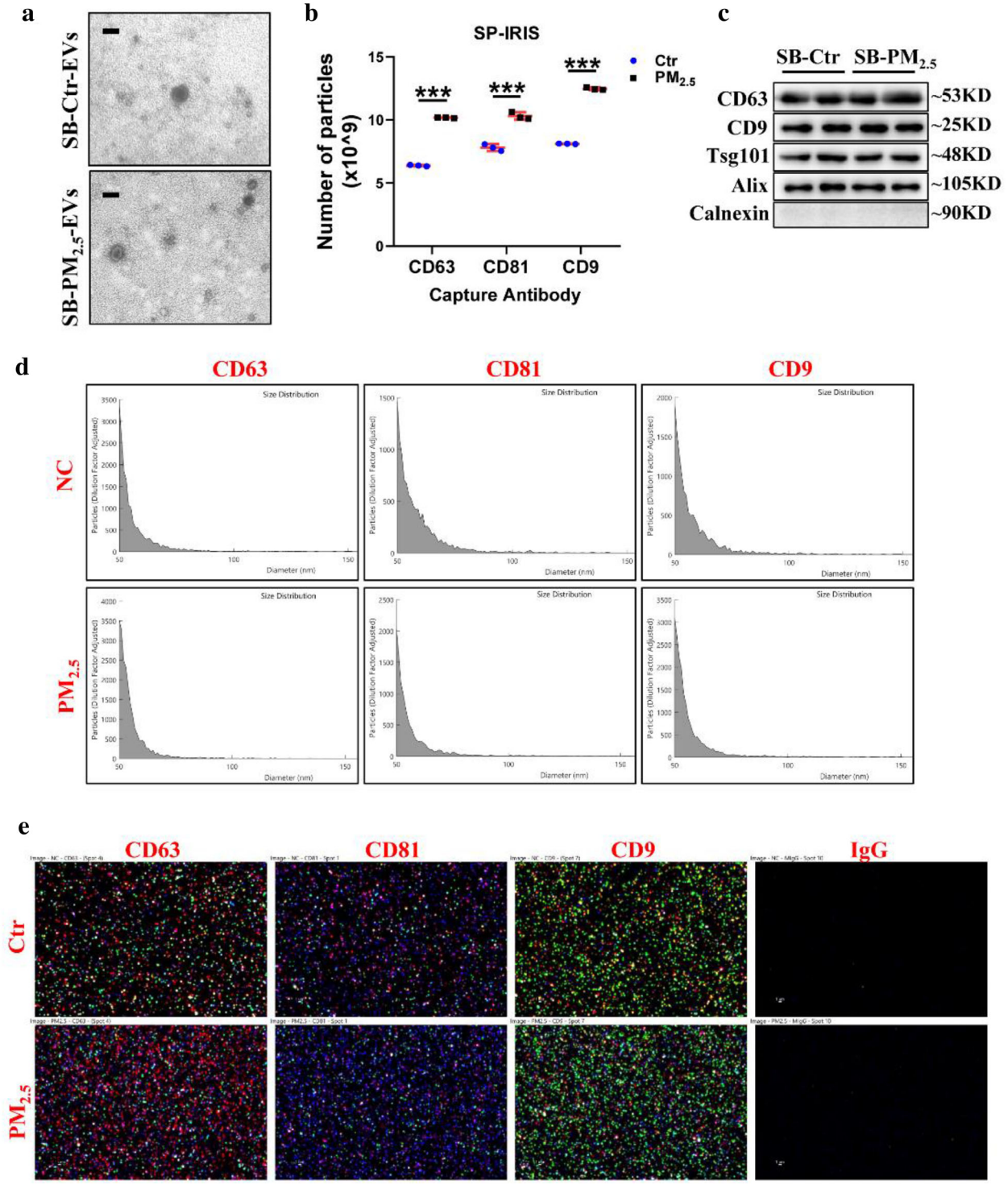

FIGURE 2 $PM_{2.5}$ exposure alters extracellular particle subpopulations. (a) The morphology of SB-ctr and SB-$PM_{2.5}$ derived EVs were displayed by TEM imaging. Scale bar = 50 nm. (b) Number of EV-marker captured subpopulations (derived from $PM_{2.5}$-exposed Beas-2B cell supernatant) were analysed by Single-Particle Interferometric Reflectance Imaging Sensor (SP-IRIS). (c) Protein marker such as CD63, CD9, Tsg101, Alix and negative marker (calnexin) were assessed by western blot. (d) Size distribution and (e) immune-colocation of EVs were performed by SP-IRIS. The chips were coated with antibodies against anti-human CD81, CD63, CD9, respectively. Anti-mouse IgG is the negative control. Fluorescent antibodies against CD81, CD63 and CD9 were used for colocation. Data were represented as mean ± SD. $n = 3$. $^{***}p < 0.001$ from comparing Ctr- and $PM_{2.5}$-exposed groups. ***SB-Ctr-EVs***: EVs derived from Beas-2B cell supernatants after exposure to PBS. ***SB -$PM_{2.5}$ -EVs***: EVs derived from Beas-2B cell supernatants after exposure to $PM_{2.5}$ for 24 h. ***SB-Ctr***: Supernatants of PBS-exposed Beas-2B cells. ***SB-$PM_{2.5}$***: Supernatants of $PM_{2.5}$-exposed Beas-2B cells

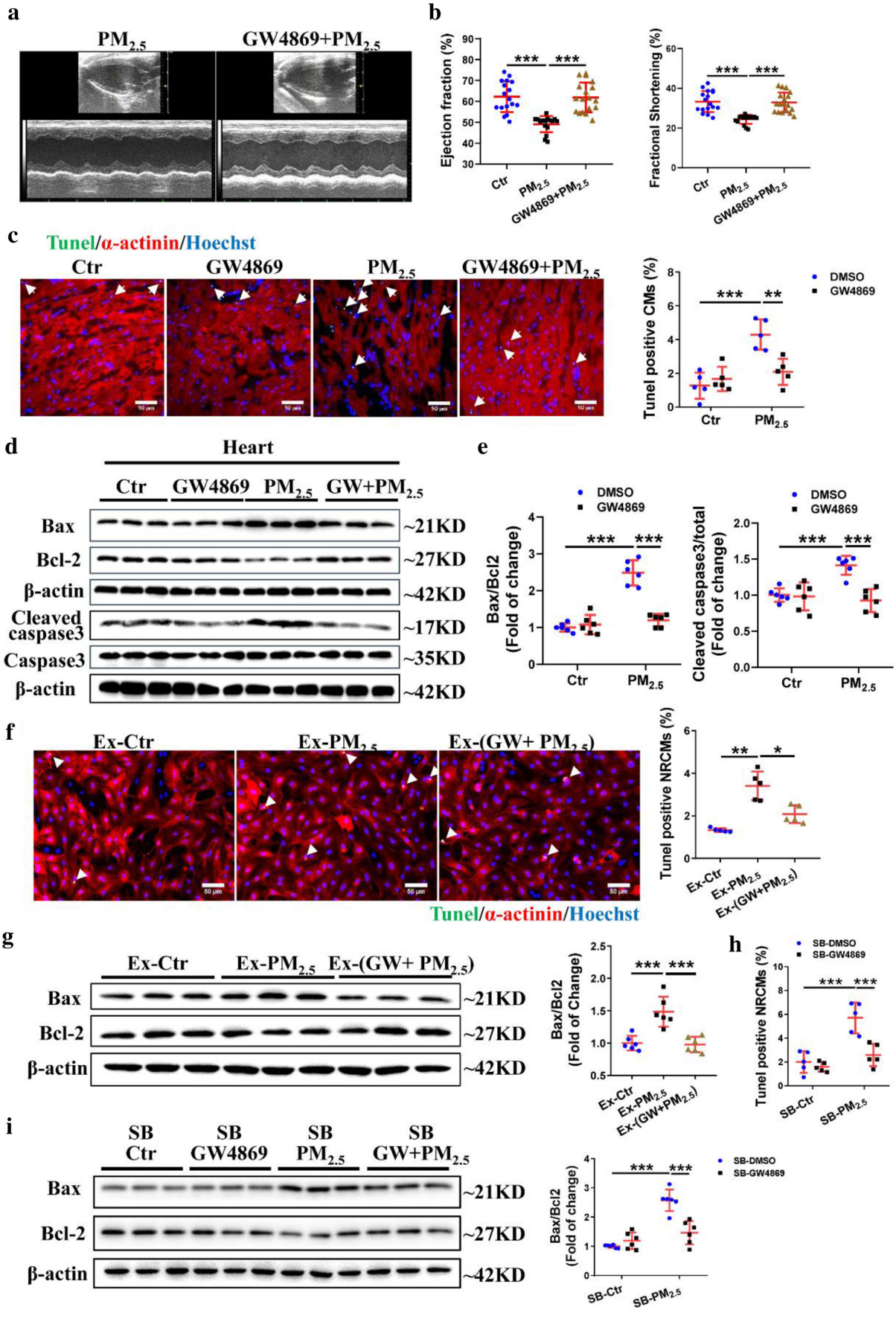
a
PM2.5
GW4869+PM2.5
b
Ejection fraction (%)
Fractional Shortening (%)
Ctr
PM2.5
GW4869+PM2.5
c
Tunel/α-actinin/Hoechst
Ctr
GW4869
PM2.5
GW4869+PM2.5
Tunel positive CMs (%)
DMSO
GW4869
d
Heart
Ctr
GW4869
PM2.5
GW+PM2.5
Bax
Bcl-2
β-actin
Cleaved caspase3
Caspase3
~21KD
~27KD
~42KD
~17KD
~35KD
e
Bax/Bcl2 (Fold of change)
Cleaved caspase3/total (Fold of change)
f
Ex-Ctr
Ex-PM2.5
Ex-(GW+ PM2.5)
Tunel positive NRCMs (%)
Tunel/α-actinin/Hoechst
g
Bax/Bcl2 (Fold of Change)
h
SB-DMSO
SB-GW4869
Tunel positive NRCMs (%)
SB-Ctr
SB-PM2.5
i
SB Ctr
SB GW4869
SB PM2.5
SB GW+PM2.5

elevating the ratio of Bax/Bcl-2, cleaved caspase 3/total caspase 3, while GW4869 attenuated cardiac apoptosis via suppressing Bax/Bcl-2 and cleaved caspase 3/total caspase 3 (Figure 3d and e).

Together, inhibition of sEV release by GW4869 could attenuate $PM_{2.5}$-induced cardiac dysfunction and cardiomyocyte apoptosis in *vivo*, suggesting a mediating effect of sEV on cardiac dysfunction post $PM_{2.5}$ exposure.

3.5 | GW4869 attenuates acute $PM_{2.5}$-induced cardiomyocyte apoptosis in vitro

To confirm the effect of pulmonary-derived sEV on cardiomyocytes apoptosis, we isolated lung, tracheal and bronchus from $PM_{2.5}$-exposed or GW4869-treated mice and cultured them ex vivo. NRCMs were exposed to ex vivo supernatant and underwent TUNEL staining. Intraperitoneal injection of GW4869 significantly attenuated Ex-$PM_{2.5}$ induced NRCMs apoptosis (Figure 3f). In line with the result of TUNEL staining, western blotting results showed that GW4869 treatment repressed Ex-$PM_{2.5}$ induced Bax/Bcl-2 increase in NRCMs (Figure 3g). These data revealed that inhibition of sEV release by GW4869 could reverse the pulmonary injury-induced cardiomyocytes apoptosis. In line with the results ex vivo, SB-$PM_{2.5}$ exposure also promoted the apoptosis of NRCMs and GW4869 treatment attenuated SB-$PM_{2.5}$-induced NRCMs apoptosis, including a reversal in TUNEL positive NRCMs numbers (Figure 3h) and Bax/Bcl-2 ratio (Figure 3i).

3.6 | Respiratory system derived sEV packaging miR-421 mediates cardiomyocytes apoptosis and cardiac dysfunction post $PM_{2.5}$ exposure

To determine which sEV-linked mediators may cause cardiomyocytes apoptosis post-$PM_{2.5}$ exposure, we explored literature and public sequencing data systematically based on biological function, circulating and EVs-packed abundance of exogenous microRNAs. We identified a well conserved, $PM_{2.5}$-associated EVs-miRNA (miR-421, 1.26 ± 0.32, $p = 0.0003$ of $PM_{2.5}$ compared to control), based on previous reports (Rodosthenous et al., 2016; Shu et al., 2015) that played important roles in regulating smoke-associated lung injury (Izzotti et al., 2011) and hypoxia-associated cardiac infarction (Liu et al., 2020; Wang et al., 2015). As shown in Figure S3, subacute respiratory exposure to $PM_{2.5}$ increased the content of miR-421 (mmu-miR421-3p) in heart tissue and serum-derived sEV (Figure S3A–S3B). To determine whether the increasing miR-421 in the heart are associated with the respiratory system, we further detected miR-421 level in $PM_{2.5}$-exposed Beas-2B cells and supernatants-derived sEV, respectively. Interestingly, our data showed that $PM_{2.5}$ exposure did not alter the content of pri-miR-421 in Beas-2B cells (Figure S3C), while reduced cellular miR-421 in Beas-2B (Figure 4a) and caused an increase in sEV-packed miR-421 (Figure 4b). Then, we used GW4869 to treat Beas-2B cells prior to $PM_{2.5}$ exposure to block sEV secretion and then collected the supernatants to treat NRCMs. SB-$PM_{2.5}$ increased miR-421 level in NRCMs whereas GW4869 pretreatment reversed $PM_{2.5}$-induced miR-421 increases (Figure 4c), suggesting that inhibiting small EVs could block $PM_{2.5}$-induced cardiac miR-421 increase in vitro. Together, these data demonstrated that $PM_{2.5}$ exposure could promote the release of miR-421 from epithelial cells to the extracellular space through sEV, which may cause cardiomyocytes apoptosis.

To investigate whether miR-421 linked EVs mediated cardiac dysfunction post-$PM_{2.5}$ exposure, we designed functional deficiency experiments in vivo and in vitro. Especially, we constructed AAV9-miR421-sponge to inhibit cardiac miR-421 in mice and investigated the role of miR-421 in $PM_{2.5}$-induced cardiac dysfunction. Briefly, mice received AAV9-miR421-sponge and its control at a dose of 10^{12}vg/mice via tail vein injection 1 day before $PM_{2.5}$ instillation (Figure 4d). The knockdown efficiency of AAV-miR421-sponge was more than 60% (Figure 4e). Compared to AAV9-Ctr group, AAV9-miR421-sponge significantly reversed EF (from 50% to 61%) and FS after $PM_{2.5}$ exposure (Figure 4f). Consistently, AAV9-miR421-sponge reduced the number of

FIGURE 3 GW4869 improves acute $PM_{2.5}$-induced cardiac dysfunction in vivo and in vitro. (a) Representative images of echocardiography measurement at day35 in $PM_{2.5}$ or $PM_{2.5}$+GW4869 treated mice. Quantitation of (b) Ejection fraction and fractional shortening ($n = 16$–18) and (c) TUNEL positive cardiomyocytes (CMs) ($n = 5$) in heart sections. Scale bar = 50μm. (d) Protein expression of Bax, Bcl-2, cleaved caspase 3 and total caspase 3 by western blot and (e) relative quantitation results of the ratio of Bax/Bcl-2, cleaved caspase 3/caspase 3 in mice heart tissues. $n = 6$. (f) Representative images of TUNEL/α-actinin/Hoechst staining in NRCMs after exposure to Ex-Ctr, Ex-$PM_{2.5}$ or Ex-($PM_{2.5}$+GW4869) for 24 h and the quantitation results of TUNEL positive NRCMs. Scale bar = 50μm. $n = 5$. (g) Protein expression of Bax and Bcl-2 after Ex-Ctr, Ex-$PM_{2.5}$ and Ex-($PM_{2.5}$+GW4869) treatment were assessed by western blot in NRCMs. $n = 6$. (h) TUNEL/α-actinin/Hoechst staining in NRCMs after exposure to SB-Ctr, SB-GW4869, SB-$PM_{2.5}$ or SB-($PM_{2.5}$+GW4869) for 24 h and TUNEL positive NRCMs were quantitated. $n = 5$. (i) Protein expression of Bax and Bcl-2 were assessed by western blot in NRCMs after exposure to SB-Ctr, SB-GW4869, SB-$PM_{2.5}$ or SB-($PM_{2.5}$+GW4869) for 24 h. $n = 6$. Data were represented as mean ± SD. $^*p < 0.05$, $^{**}p < 0.01$ and $^{***}p < 0.001$, respectively, from comparing control- and $PM_{2.5}$-exposed groups. p-values were calculated by one way (b, f, g) or two-way ANOVA (c, e, h and i) with Tukey correction for multiple comparisons. ***Ex-Ctr***: ex vivo culture supernatants of PBS-exposed mice lung and bronchi. ***Ex-$PM_{2.5}$***: ex vivo culture supernatants of $PM_{2.5}$-exposed mice lung and bronchi. ***Ex-(GW+$PM_{2.5}$)***: GW4869 were administrated to mice for 2 hours prior to exposure to $PM_{2.5}$. Separating the lungs and bronchi from these mice at day15 for 48 h and then collected the supernatants. ***SB-Ctr***: Supernatants of PBS-exposed Beas-2B cells. ***SB-$PM_{2.5}$***: Supernatants of $PM_{2.5}$-exposed Beas-2B cells. ***SB-GW4869***: Supernatants of GW4869 treated Beas-2B cells. ***SB-(GW+$PM_{2.5}$)***: Beas-2B cells were pretreated with GW4869 and then exposed to $PM_{2.5}$ for 24 h. Collecting the supernatants for use

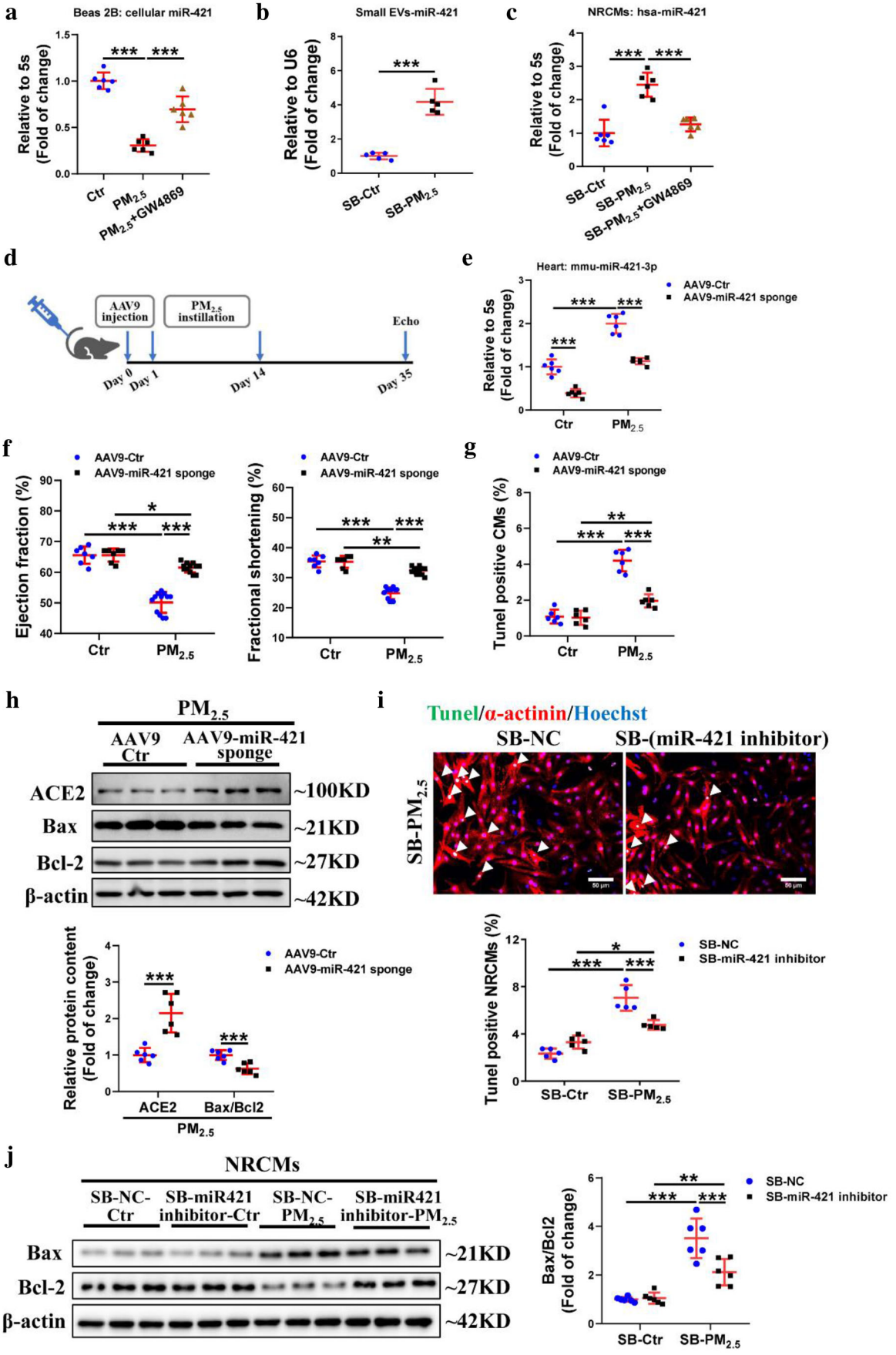
a
Beas 2B: cellular miR-421
Relative to 5s (Fold of change)
Ctr
PM2.5
PM2.5+GW4869
b
Small EVs-miR-421
Relative to U6 (Fold of change)
SB-Ctr
SB-PM2.5
c
NRCMs: hsa-miR-421
Relative to 5s (Fold of change)
SB-Ctr
SB-PM2.5
SB-PM2.5+GW4869
d
AAV9 injection
PM2.5 instillation
Echo
Day 0
Day 1
Day 14
Day 35
e
Heart: mmu-miR-421-3p
AAV9-Ctr
AAV9-miR-421 sponge
Relative to 5s (Fold of change)
Ctr
PM2.5
f
AAV9-Ctr
AAV9-miR-421 sponge
Ejection fraction (%)
Fractional shortening (%)
Ctr
PM2.5
g
AAV9-Ctr
AAV9-miR-421 sponge
Tunel positive CMs (%)
Ctr
PM2.5
h
PM2.5
AAV9 Ctr
AAV9-miR-421 sponge
ACE2
Bax
Bcl-2
β-actin
~100KD
~21KD
~27KD
~42KD
AAV9-Ctr
AAV9-miR-421 sponge
Relative protein content (Fold of change)
ACE2
Bax/Bcl2
PM2.5
i
Tunel/α-actinin/Hoechst
SB-NC
SB-(miR-421 inhibitor)
SB-PM2.5
SB-NC
SB-miR-421 inhibitor
Tunel positive NRCMs (%)
SB-Ctr
SB-PM2.5
j
NRCMs
SB-NC-Ctr
SB-miR421 inhibitor-Ctr
SB-NC-PM2.5
SB-miR421 inhibitor-PM2.5
Bax
Bcl-2
β-actin
~21KD
~27KD
~42KD
SB-NC
SB-miR-421 inhibitor
Bax/Bcl2 (Fold of change)
SB-Ctr
SB-PM2.5

TUNEL positive cardiomyocytes (Figure 4g) and Bax/Bcl-2 ratio (Figure 4h), suggesting a protective role of miR421 knockdown in $PM_{2.5}$-inuced cardiomyocyte apoptosis.

To assess the potential therapeutical effect of pulmonary miR-421 inhibition in vitro, we suppressed miR-421 in Beas-2B cells prior to $PM_{2.5}$ exposure and then collected the supernatants to treat NRCMs. Inhibition of miR-421 in Beas-2B cells attenuated SB-$PM_{2.5}$ induced NRCMs apoptosis, including a reduced TUNEL positive NRCMs (Figure 4i) and a reduced ratio of Bax/Bcl-2 (Figure 4j) in SB-miR-421-inhibitor-$PM_{2.5}$ group compared to SB-NC-$PM_{2.5}$.

These data demonstrated that pulmonary $PM_{2.5}$ exposure caused cardiac dysfunction by promoting sEV-miR421 transfer to cardiomyocytes. Inhibition of pulmonary-derived sEV-miR-421 via GW4869 or AAV9-miR421-sponge could attenuate $PM_{2.5}$-induced cardiac dysfunction and cardiomyocytes apoptosis.

3.7 | sEV-miR421 suppresses ACE2 in heart and cardiomyocytes

To explore the downstream mediators of sEV-miR421 function, we used bioinformatics prediction through miRDB database and based our selection on subsequent literature searches. Among potential target genes, angiotensin converting enzyme 2 (ACE2) is well-known to be associated with cardiovascular homeostasis. Especially, miR-421 inhibits the expression of ACE2 in primary fibroblasts from patient' hearts with coronary artery bypass surgery (Lambert et al., 2014). Based on the bioinformatics prediction results (Figure 5a), we performed luciferase reporter assays in 293T containing the ACE2 3′-UTR or mutant controls. Transfection with miR-421 mimics but not their negative controls caused a significant decrease in luciferase expression. In addition, miR-421 mimics inhibited the luciferase expression in ACE2 3′-UTR but not its mutant control, providing direct evidence that ACE2 3′-UTR is the binding site of miR-421 (Figure 5b). Subacute respiratory $PM_{2.5}$ exposure significantly suppressed the expression of ACE2 in mice hearts and GW4869 reversed the ACE2 levels in vivo (Figure 5c) and ex vivo (Figure 5d). Inhibition of sEV release from Beas-2B cells by GW4869 blocked SB-$PM_{2.5}$ induced ACE2 reduction in vitro (Figure 5e). We then suppressed cellular miR-421 by using miR-421 inhibitor in Beas-2B cells and collected the supernatants for subsequent NRCMs exposure. Inhibition of miR-421 in Beas-2B reversed SB-$PM_{2.5}$ induced ACE2 reduction (Figure 5f). In addition, we performed functional reversal experiment by inhibiting the expression of ACE2 in NRCMs, prior to exposing to SB-$PM_{2.5}$ (at the existence of miR-421 inhibitor or NC). Inhibition of miR-421 in Beas-2B reversed SB-$PM_{2.5}$-induced cardiomyocytes apoptosis and ACE2 downregulation. However, inhibition of the expression of ACE2 blocked the protective roles of miR-421 silence on SB-$PM_{2.5}$-induced NRCMs apoptosis (Figure 5g).

All these data suggested that cardiac ACE2 was a downstream target of pulmonary sEV-miR-421, which plays crucial roles in mediating $PM_{2.5}$-induced cardiomyocytes apoptosis and cardiac dysfunction.

To validate the role of ACE2 in $PM_{2.5}$-sEV mediated cardiac dysfunction, siRNAs were transfected in NRCMs to inhibit the expression of ACE2. Inhibition of ACE2 robustly increased TUNEL positive NRCMs (Figure S4A and S4B) and the ratio of Bax/Bcl-2 (Figure S4C) in basal states, while no longer a deterioration in the Ex-$PM_{2.5}$ group was visible (Figure S4A–S4C). Furthermore, silence of ACE2 also caused an increase in TUNEL positive NRCMs (Figure S4D–S4E) and Bax/Bcl-2 ratio (Figure S4F) in the SB-Ctr group, while no differences in SB-$PM_{2.5}$ exposed group was present. All these data suggested that ACE2 deficiency could cause cardiomyocytes apoptosis in basal state, whose deficiency may contribute to $PM_{2.5}$-induced cardiomyocyte apoptosis.

FIGURE 4 Respiratory system derived sEV packaging miR-421 mediates cardiomyocytes apoptosis after $PM_{2.5}$ exposure. Relative content of hsa-miR-421 in (a) Beas-2B cells, (b) small EVs derived from the supernatants of Beas-2B and (c) NRCMs. $n = 5$–6. 5S and U6 were used as internal control of cellular miR-421 and sEV-contained miR-421, respectively. (d) Schematic representation of experimental design in vivo. To investigate the effect of miR-421 in $PM_{2.5}$-induced cardiac dysfunction in vivo, AAV9-miR421-sponge and its control (AAV9-Ctr) were utilised to inject into mice followed by $PM_{2.5}$ exposure. Echocardiography (Echo) measurement were performed at day35. (e) The knockdown efficiency of mmu-miR421-3p in heart was examined by Realtime PCR and 5S was used as the control. $n = 6$. (f) The ejection fraction and fractional shortening of heart at day35 were shown. $n = 7,7,12,12$. (g) Quantitation of TUNEL positive cardiomyocytes were analysed in AAV9-Ctr or AAV9-miR421-sponge injected mice heart with or without $PM_{2.5}$ exposure. $n = 6$. (h) The expression of ACE2 and Bax/Bcl-2 were examined in $PM_{2.5}$-exposed AAV9-Ctr or AAV9-miR421-sponge injected mice heart. $n = 6$. (i) The NRCMs were exposed to SB-NC-Ctr, SB-miR-421inhibitor-Ctr, SB-(NC+$PM_{2.5}$) or SB-(miR-421 inhibitor+$PM_{2.5}$) for 24 h and then received TUNEL/α-actinin/Hoechst staining (Scale bar = 50 μm) and TUNEL positive NRCMs were quantitated. $n = 5$. (j) The protein expression of Bax and Bcl-2 were assessed by western blot and quantitated by Image J. n = 6. Data were represented as mean ± SD. $^*p < 0.05$, $^{**}p < 0.01$ and $^{***}p < 0.001$, respectively. *p*-values were calculated by unpaired Student's *t*-test (b, h), one-way ANOVA (a, c), two-way ANOVA with Tukey correction (e, f, g, i and j) for multiple comparisons. ***SB-Ctr***: Supernatants of PBS-exposed Beas-2B cells. ***SB-PM$_{2.5}$***: Supernatants of $PM_{2.5}$-exposed Beas-2B cells. ***SB-NC-Ctr***: Beas-2B cells were transfected with negative control siRNA followed by exposure to fresh PBS/DMEM and the supernatants were collected. ***SB-miR421 inhibitor-Ctr***: Beas-2B cells were transfected with miR-421 inhibitor followed by exposure to fresh PBS/DMEM and the supernatants were collected. ***SB-NC-PM$_{2.5}$***: Beas-2B cells were transfected with negative control siRNA followed by exposure to $PM_{2.5}$ for 24 h and the supernatants were collected. ***SB-miR421 inhibitor-PM$_{2.5}$***: Beas-2B cells were transfected with miR-421 inhibitor followed by exposure to $PM_{2.5}$ for 24 h and the supernatants were collected

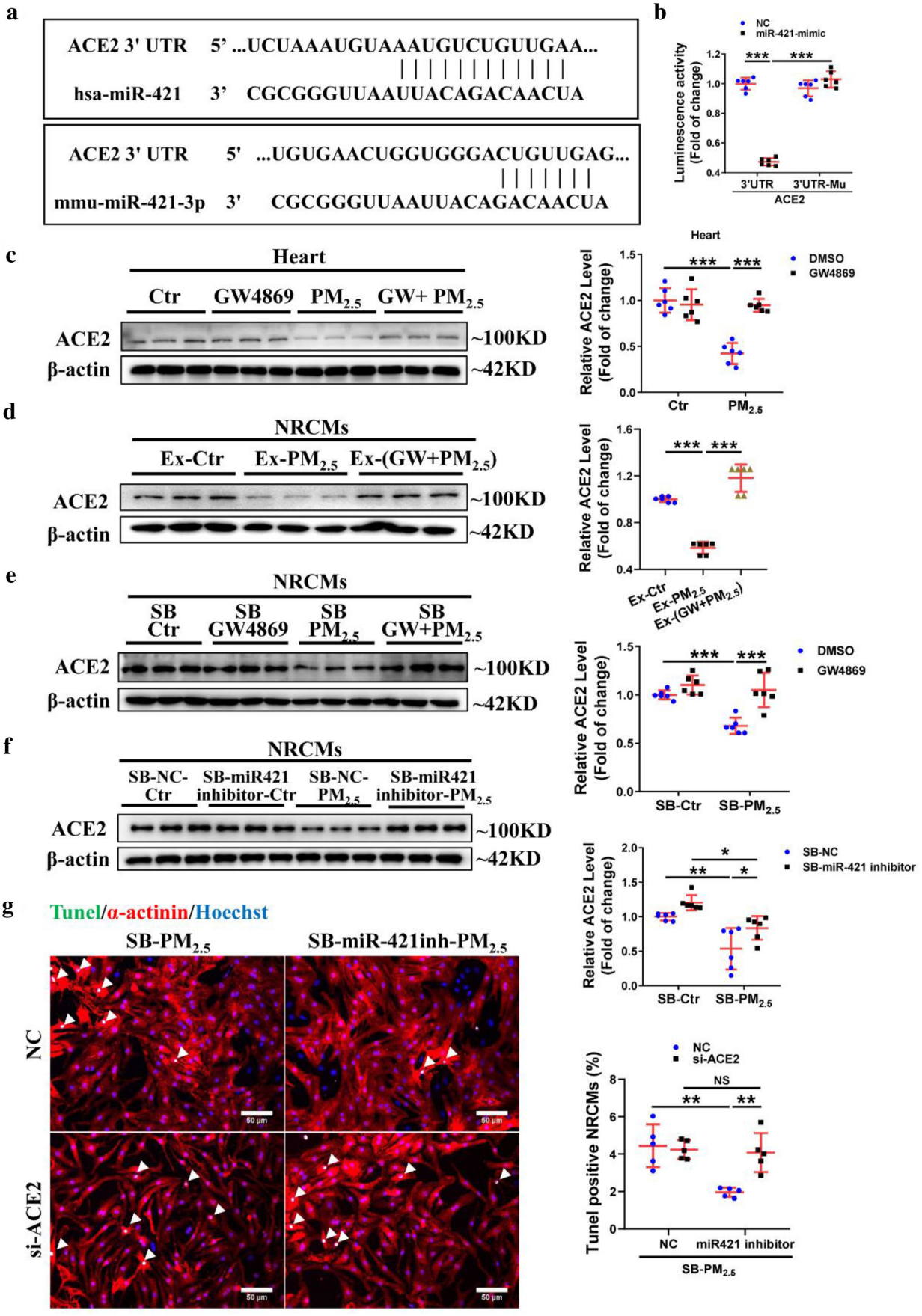
a
ACE2 3' UTR 5' ...UCUAAAUGUAAAUGUCUGUUGAA...
hsa-miR-421 3' CGCGGGUUAAUUACAGACAACUA
ACE2 3' UTR 5' ...UGUGAACUGGUGGGACUGUUGAG...
mmu-miR-421-3p 3' CGCGGGUUAAUUACAGACAACUA
b
NC
miR-421-mimic
Luminescence activity (Fold of change)
3'UTR
3'UTR-Mu
ACE2
c
Heart
Ctr
GW4869
PM2.5
GW+ PM2.5
ACE2
β-actin
~100KD
~42KD
Relative ACE2 Level (Fold of change)
DMSO
GW4869
d
NRCMs
Ex-Ctr
Ex-PM2.5
Ex-(GW+PM2.5)
e
SB Ctr
SB GW4869
SB PM2.5
SB GW+PM2.5
f
SB-NC-Ctr
SB-miR421 inhibitor-Ctr
SB-NC-PM2.5
SB-miR421 inhibitor-PM2.5
SB-Ctr
SB-PM2.5
SB-NC
SB-miR-421 inhibitor
g
Tunel/α-actinin/Hoechst
SB-PM2.5
SB-miR-421inh-PM2.5
NC
si-ACE2
50 μm
Tunel positive NRCMs (%)
NS
miR421 inhibitor

3.8 | Overexpression of ACE2 attenuates $PM_{2.5}$-induced cardiomyocytes apoptosis ex vivo and in vitro

We increased the expression of ACE2 by transfecting overexpressing human ACE2 plasmids (OE-hACE2) or scramble controls (Scr) into NRCMs. Apoptosis assessment showed that overexpression of ACE2 could not alter the cell viability in basal conditions comparing to scramble controls, while reducing TUNEL positive NRCMs (Figure 6a and b) and Bax/Bcl-2 ratio (Figure 6c) in SB-$PM_{2.5}$ group. In compliance with the in vitro results, overexpression of ACE2 attenuated Ex-$PM_{2.5}$ induced increasing in TUNEL positive NRCMs (Figure S5A and S5B), as well as the ratio of Bax/Bcl-2 (Figure S5C). Together, elevating the expression of ACE2 could protect cardiomyocytes against $PM_{2.5}$-induced cell apoptosis.

3.9 | DIZE inhibits respiratory $PM_{2.5}$ exposure-induced cardiac dysfunction and cardiomyocytes apoptosis

To explore a potential therapeutical strategy for $PM_{2.5}$-induced cardiomyocytes apoptosis and cardiac dysfunction, DIZE, an established activator of ACE2, was injected in mice. The procedure of DIZE treatment as well as $PM_{2.5}$ exposure in vivo was shown as Figure S6A. Cardiac function was assessed by echocardiography measurement 30-day post injection of DIZE. DIZE administration reversed the $PM_{2.5}$-induced EF and FS reduction (Figure 6d), demonstrating an improvement of cardiac function after DIZE treatment. TUNEL staining data displayed that DIZE administration caused a significant reduction in $PM_{2.5}$-induced cardiomyocytes apoptosis in mice hearts (Figure S6B). In compliance with the TUNEL data, apoptotic-associated proteins assessment indicated that DIZE caused an increase in ACE2 expression and reduced the ratio of Bax/Bcl-2 as well as cleaved-caspase 3/total caspase 3 in $PM_{2.5}$-exposed mice (Figure 6e).

To further confirm the role of DIZE treatment in $PM_{2.5}$-induced cardiomyocyte apoptosis, we also performed functional experiments in NRCMs in vitro. In SB-$PM_{2.5}$ exposed NRCMs, TUNEL staining showed that DIZE treatment caused a significant reduction in TUNEL-positive NRCMs (Figure S6C). Apoptotic protein assessment by western blot showed that DIZE could upregulate ACE2 expression and suppress Bax/Bcl-2 and cleaved caspase 3/total caspase 3 after SB-$PM_{2.5}$ exposure (Figure S6D), which demonstrated a reduced cardiomyocytes apoptosis induced by DIZE treatment after $PM_{2.5}$ exposure.

All together, DIZE treatment attenuated subacute $PM_{2.5}$ exposure-induced cardiac dysfunction and cardiomyocytes apoptosis via improving ACE2 expression, which may be a potential therapeutical strategy for air pollution related CVD.

3.10 | ACE2 suppresses iNOS expression after $PM_{2.5}$ exposure

Of note, since ACE2 is an important regulator of blood pressure (BP), we assessed systolic blood pressure (SBP) and diastolic blood pressure (DBP) in mice. $PM_{2.5}$ exposure caused a significant increase in SBP, DBP and mean BP compared to control group, while DIZE administration attenuated $PM_{2.5}$-induced high BP (Figure S7A), suggesting a possible involvement of endothelium. Therefore, markers of endothelial injury such as endothelial nitric oxide synthase (eNOS) and iNOS was detected. Our data showed that $PM_{2.5}$ exposure did not alter the expression of cardiac eNOS (Figure S7B), while promoting the expression of cardiac iNOS (Figure S7C). Same conclusion was drawn in HUVEC (Figure S7D and S7E). These data inspire us to assess the content

FIGURE 5 sEV-miR421 targets cardiac ACE2 and mediates $PM_{2.5}$-induced cardiomyocytes apoptosis. (a) The bioinformatics prediction results for downstream of miR-421 in human and mice through miRDB database. (b) To verify the binding site between miR-421 and ACE2, we constructed luciferase reporter gene with higher luminescence in the ACE2 3′-UTR and then cotransfected with miR-421 mimic, which caused a significant decrease in the expression of luciferase. However, miR-421 mimic has no effect on ACE2 3′-UTR mutant luciferase expression. $n = 6$. (c) The protein expression of ACE2 in mice heart were assessed by western blot at day36. GW4869 were administrated to mice via intraperitoneal injection every other day. $n = 6$. The protein expression of ACE2 in NRCMs after exposure to (d) Ex-Ctr, Ex-$PM_{2.5}$ or Ex-($PM_{2.5}$+GW4869) as well as (e) SB-Ctr, SB-GW4869, SB-$PM_{2.5}$ or SB-($PM_{2.5}$+GW4869). $n = 6$. (f) Relative ACE2 expression in NRCMs after exposure to SB-NC-Ctr, SB-miR421 inhibitor-Ctr, SB-NC-$PM_{2.5}$ or SB-miR421 inhibitor-$PM_{2.5}$. $n = 6$. (g) Functional reverse experiment of miR-421 in vitro. NRCMs were transfected with si-ACE2 or negative control and then exposed to SB-$PM_{2.5}$ or SB-miR421 inhibitor-$PM_{2.5}$ for 24 h. Subsequently, NRCMs apoptosis was assessed by TUNEL staining combined with α-actinin/Hoechst staining. $n = 5$. Data were represented as mean ± SD. $^*p < 0.05$, $^{**}p < 0.01$ and $^{***}p < 0.001$, respectively. p-values were calculated by one-way ANOVA with Tukey correction (d) or two-way ANOVA with Tukey correction (b, c, e, f and g) for multiple comparisons. *Ex-Ctr*: ex vivo culture supernatants of PBS-exposed mice lung and bronchi. *Ex-$PM_{2.5}$*: ex vivo culture supernatants of $PM_{2.5}$-exposed mice lung and bronchi. *Ex-(GW+$PM_{2.5}$)*: GW4869 were administrated to mice and then exposed to $PM_{2.5}$. Separating the lungs and bronchi from these mice at day15 for 48 h and then collected the supernatants. ***SB-Ctr***: Supernatants of PBS-exposed Beas-2B cells. ***SB-$PM_{2.5}$***: Supernatants of $PM_{2.5}$-exposed Beas-2B cells. ***SB-GW4869***: Supernatants of GW4869 treated Beas-2B cells. ***SB-(GW+$PM_{2.5}$)***: Beas-2B cells were pretreated with GW4869 and then exposed to $PM_{2.5}$ for 24 h. Collecting the supernatants and centrifugating removal of pallets for use. ***SB-NC-Ctr***: Beas-2B cells were transfected with negative control siRNA followed by exposure to fresh PBS/DMEM and the supernatants were collected and centrifugated. ***SB-miR421 inhibitor-Ctr***: Beas-2B cells were transfected with miR-421 inhibitor followed by exposure to fresh PBS/DMEM and the supernatants were collected. ***SB-NC-$PM_{2.5}$***: Beas-2B cells were transfected with negative control siRNA followed by exposure to $PM_{2.5}$ for 24 h and the supernatants were collected. ***SB-miR421 inhibitor-$PM_{2.5}$***: Beas-2B cells were transfected with miR-421 inhibitor followed by exposure to $PM_{2.5}$ for 24 h and the supernatants were collected. ***Si-ACE2***: ACE2-siRNA

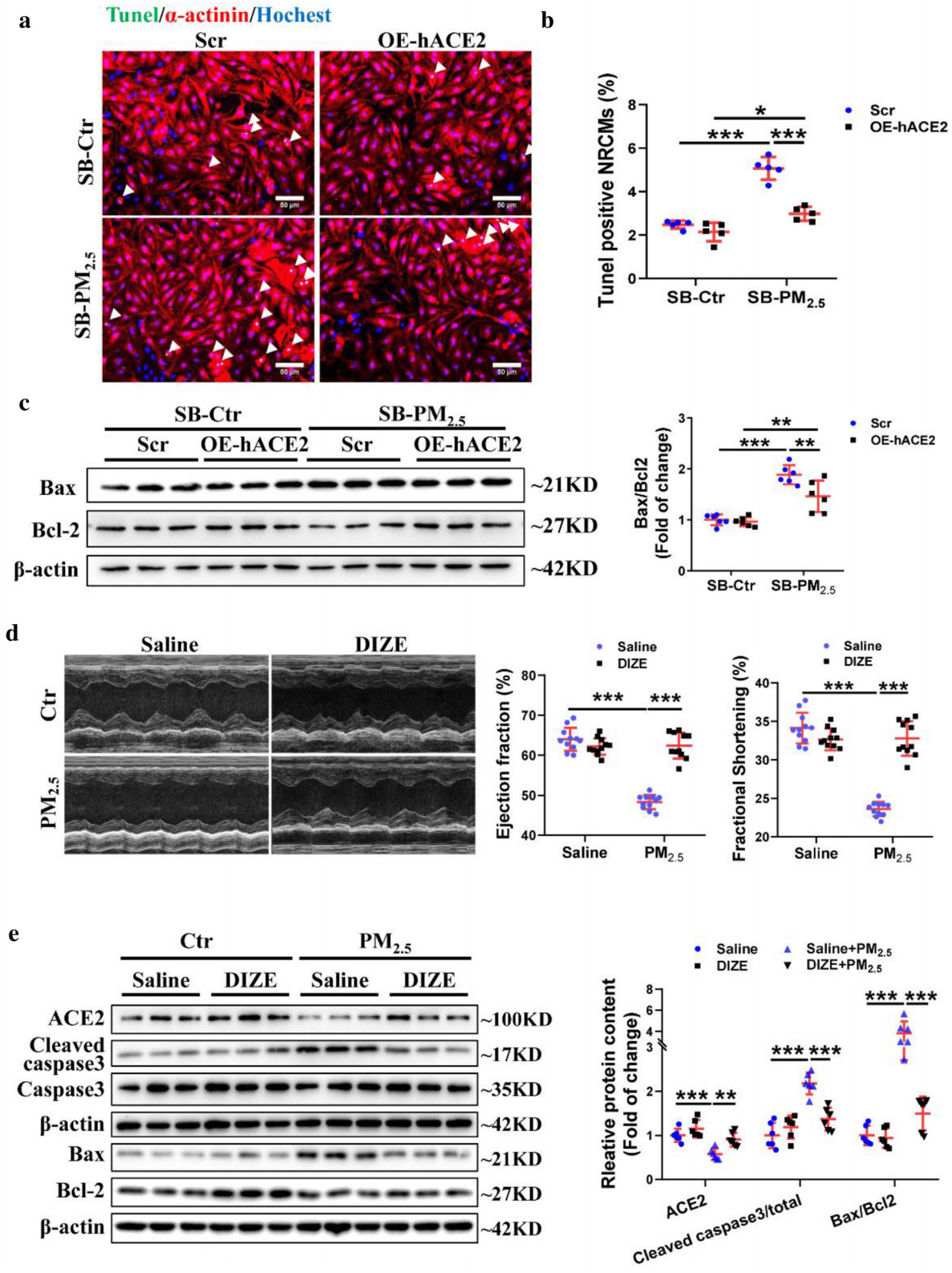

FIGURE 6 Upregulation of ACE2 attenuates $PM_{2.5}$-induced cardiomyocytes apoptosis in vitro and in vivo. NRCMs were transfected with over expressed-human ACE2 (OE-hACE2) or scramble control (Scr) followed by exposure to SB-Ctr or SB-$PM_{2.5}$ for 24 h respectively and then received TUNEL/α-actinin/Hoechst staining. (a) Representative images of TUNEL staining and (b) quantitation of TUNEL positive NRCMs. Scale bar = 50 μm. $n = 5$. (c) NRCMs were transfected with OE-hACE2 or scramble control followed by exposure to SB-Ctr or SB-$PM_{2.5}$ for 24 h respectively and relative expression of Bax and Bcl-2 were assessed by western blot. $n = 6$. Diminazene aceturate (DIZE) was used to reveal the effect of ACE2 activation on $PM_{2.5}$-induced cardiac dysfunction. Cardiac function was examined by echocardiography at day35. (d) Representative images of cardiac function were obtained by echocardiography, and cardiac ejection fraction and fraction shorting were quantified. $n = 11$. (e) The protein expression of ACE2, Bax, Bcl-2, cleaved caspase 3 and caspase 3 in heart tissue lysates of mice. $n = 6$. Data were represented as mean ± SD. $^*p < 0.05$, $^{**}p < 0.01$ and $^{***}p < 0.001$. p-values were calculated by two-way ANOVA with Tukey correction for multiple comparisons

of iNOS in cardiomyocytes to figure out the original reason of cardiomyocyte apoptosis. As shown in Figure S8A, activation of ACE2 by DIZE can inhibit the increase of cardiac iNOS after $PM_{2.5}$ exposure. We further performed experiment to investigate the regulatory effect between ACE2 and iNOS in NRCMs. Inhibition of iNOS by L-NAME did not alter the content of ACE2 under SB-$PM_{2.5}$ condition (Figure S8B). Together, these data demonstrated that iNOS was suppressed by ACE2, whose alteration may mediate the toxicity of $PM_{2.5}$ on endothelial cells and cardiomyocytes.

4 | DISCUSSION

Although previous evidence demonstrates that exposure to particulate pollution contributes to the development of CVD (Bai et al., 2019; Hayes et al., 2020; Madrigano et al., 2013), the mechanistic basis of this process is not fully elucidated. In this study, we observed cardiac dysfunction secondary to pulmonary damage after subacute exposure to ambient $PM_{2.5}$, having a cardiac deterioration that was time-dependent in vivo. Especially, we identified that pulmonary derived small EVs could transfer miR-421 and target cardiac ACE2, which mediates $PM_{2.5}$-induced cardiomyocytes apoptosis and cardiac dysfunction ex vivo and in vitro. Furthermore, inhibition of EVs secretion, downregulation of miR-421 content or activation of ACE2 can attenuate $PM_{2.5}$-induced cardiomyocytes apoptosis and cardiac dysfunction, which would be potential therapeutical strategies for treating air pollution related CVD.

Some epidemiology studies show that acute, short-term of $PM_{2.5}$ exposure is associated with increased CVD hospitalisation (Qiu et al., 2020), especially for heart failure admissions (Stafoggia et al., 2020). Cardiac troponin T assessment demonstrates that acute PM exposure may elevate myocardial damage (Zhang et al., 2021). However, short-term air pollution exposure does not influence arterial stiffness (Ljungman et al., 2018). To investigate the role of short-term $PM_{2.5}$ exposure via respiratory system on cardiac function, we established a $PM_{2.5}$ exposure model at a short-term adjust upon previous research (Gao et al., 2020; Liu et al., 2021). Surprisingly, we found that cardiac function gradually decreased post $PM_{2.5}$ exposure with time preceding, demonstrating a potential cross talk occurring between lungs and heart. To confirm the existence of an induced cross talk by $PM_{2.5}$, we further performed organ culture ex vivo and bronchial epithelial cells culture in vitro and then collect the supernatants to treat cardiomyocytes. Ex vivo and in vitro experiments strengthen the hypothesis that cross talk from lungs to heart occurred in response to $PM_{2.5}$ exposure.

EVs are considered as important messengers in mediating intercellular communication, which plays crucial roles in several pathological processes. However, the effect of $PM_{2.5}$ exposure on particle subpopulation changes is still unclear. Therefore, we investigated extracellular subpopulation changes in response to $PM_{2.5}$ in vitro through SP-IRIS and revealed that $PM_{2.5}$ exposure caused a significant increase in CD63, CD81 and CD9 colocalisation of small EVs compared to control groups, which may lay a foundation for exploring $PM_{2.5}$-associated EV subpopulations. Actually, further verification of the major cargo among these subpopulations in vivo is still needed. Revealing the specific subpopulation of EV mediating cross talk is crucial to illuminate the biological mechanism of $PM_{2.5}$-induced toxicity in vivo, which will be significative. In the present study, since we reveal that EVs containing miR-421 mediates lungs to heart cross talk after $PM_{2.5}$ exposure, we performed GW4869 administration to mice to explore the therapeutical effect. GW4869 administration attenuated $PM_{2.5}$-induced cardiomyocyte apoptosis and cardiac dysfunction, which may be a potential strategy for air pollution-related CVD treatment.

To date, multiple causes are considered be associated with high dose or long-term exposure to $PM_{2.5}$-induced cardiac injury such as oxidative stress (Gangwar et al., 2020; Wang et al., 2018) and inflammation (Abohashem et al., 2021). Prolonged exposure to particulate pollution is identified to cause endothelial and systematic inflammation (Pope et al., 2016) and epigenetic changes (Madrigano et al., 2011), which may contribute to cardiac injury. Although short-term $PM_{2.5}$ exposure robustly increased pulmonary inflammation and oxidative stress (Sun et al., 2020; Yue et al., 2019), little studies revealed the mechanism of cardiac dysfunction after lung injury. Furthermore, it was reported that no changes of systemic inflammatory factors were observed in previous study (Davel et al., 2012). Therefore, inflammatory reaction is complex in the toxicity of $PM_{2.5}$, which needs specific observation depends on different situation. In the present study, to confirm whether pulmonary inflammation and oxidative stress are associated with short-term exposure of $PM_{2.5}$-induced cardiac dysfunction, we assess inflammatory factors level in heart tissues. We did not find significant differences between $PM_{2.5}$-exposed and PBS exposed hearts, which may be a result of an adaptive increase in nuclear factor E2-related factor 2 (Nrf2) and anti-inflammatory factors post $PM_{2.5}$ exposure upon previous studies in vivo (Xu et al., 2017) and in vitro (Deng et al., 2013; Wang et al., 2016).

ACE2, the homologue of angiotensin-converting enzyme, plays crucial roles in the renin-angiotensin system of the heart (Donoghue et al., 2000). In the heart, ACE2 has been identified to be expressed in endothelial cells, smooth muscle cells and cardiomyocytes (Burrell et al., 2005). Increasing evidence demonstrate that ACE2 plays essential roles in regulating cardiac function and whose disruption can cause cardiac contractility defect (Crackower et al., 2002). Therefore, increased expression or enzyme activity of ACE2 are found effective in counteracting diseases including CVD. A previous study revealed that enhancing ACE2 may be a novel therapy for patients with heart failure (Patel et al., 2016). In the present study, we found that activating ACE2 by DIZE, an activator of ACE2, could protect the mice against $PM_{2.5}$-induced cardiac dysfunction. In addition, we also identified a regulator of ACE2, EV-containing miR-421, whose reduction attenuates $PM_{2.5}$-induced cardiomyocytes apoptosis

via post-transcriptional regulation of ACE2. The regulating mechanism of miR-421 on ACE2 in our study was consist with previous research (Lambert et al., 2014). Notably, inhibiting miR-421 flux via AAV9-miR421-sponge significantly improves cardiac EF from 50% to 61% after $PM_{2.5}$ exposure, suggesting a protective role of miR-421 knockdown.

Several studies indicate that $PM_{2.5}$ exposure can cause an increase in iNOS or NO production (Chen et al., 2015; Guo et al., 2019), whose increase is associated with $PM_{2.5}$-induced vascular dysfunction (Long et al., 2020) and cell apoptosis (Wang et al., 2016). Therefore, we investigated the regulatory relationship of ACE2 and iNOS in $PM_{2.5}$-induced cardiomyocytes apoptosis in vitro. We found that inhibition of iNOS did not alter the expression of ACE2, while DIZE can suppress the iNOS expression. It matters important to examine the effect of L-NAME in $PM_{2.5}$-induced cardiac injury in vivo in the future.

According to a previous study, short-term exposure to ultrafine PM is associated with blood pressure changes in adults (Van Nunen et al., 2021). To confirm whether blood pressure is associated with ACE2-induced cardioprotection after $PM_{2.5}$ exposure, we assessed the BP after $PM_{2.5}$ exposure in mice and revealed that activating ACE2 by DIZE can attenuate $PM_{2.5}$-indcued SBP and DBP increase, demonstrating BP-regulation mechanism induced by ACE2 is associated with $PM_{2.5}$-induced cardiac dysfunction.

However, we cannot exclude the possibility that $PM_{2.5}$-induced sEV mediates cross talk between other organs and the heart post lung injury. Metabolic influence is also an important process involved in $PM_{2.5}$-associated outcomings. Several evidence showed that $PM_{2.5}$ exposure could alter the concentration of metabolites in plasma (Breitner et al., 2016) and the composition of gut microbiota (Liu et al., 2021). Further studies need to perform to investigate the cross talk between lung-gut microbiota-heart in response to $PM_{2.5}$. Previous evidence showed that $PM_{2.5}$ exposure can alter pulmonary microbiome composition and disturbed metabolic pathways (Li et al., 2020). Therefore, whole body exposure system is better to mimic the inhalational toxicity of $PM_{2.5}$ compared to intratracheal instillation, which is a limitation of our present study. However, it is difficult to assess the actual dose (not natural concentration) of particles inhaled into the respiratory system in whole body exposure system; Alternatively, the majority of the inhalable microorganisms in Beijing's $PM_{2.5}$ and PM_{10} pollutants were soil-associated and nonpathogenic to human (Cao et al., 2014) (>400 citations). Therefore, we utilized intratracheal instillation with exact dose to build subacute $PM_{2.5}$ exposure model. Our conclusion needs to be further verified through whole body exposure system in the future.

Of note, multiple cells may participate in $PM_{2.5}$-induced cardiac dysfunction, including macrophage, epithelial and endothelial cells, etc. The actual role of different cell population in $PM_{2.5}$-induced cardiac injury needs to be further investigated. Here we reveal that the respiratory system, especially bronchial epithelial cells derived sEV, contributes to cardiac dysfunction induced by $PM_{2.5}$ exposure. Especially, macrophages are known playing crucial role in $PM_{2.5}$-induced lung inflamamtion (He et al., 2017), while their role in mediating cross talk to cardiomyocytes are still unknown and deserves further investigation in the future. We found that cell numbers in BALF, TNF-α and oxidative stress increased in $PM_{2.5}$-exposed lung tissue, indicating macrophage, neutrophils and epithelial cells involved in lung inflammation in our model. Nevertheless, different from lung tissue, we did not find a significant increase of inflammatory reaction in heart tissues (Figure S2), indicating a way independent of inflammation occurred in our model. Given the priority of endothelial cells in uptake EVs from the bloodstream, the effect of endothelial cells during the cross talk should be investigated. Especially, whether the soluble component of $PM_{2.5}$ particles directly influence endothelial function in vivo and how long does $PM_{2.5}$ particles last in pulmonary tissue are still challenging because of the difficulty of $PM_{2.5}$ tracking.

In conclusion, we revealed for the first time that cardiac dysfunction is secondary to pulmonary injury and is time-dependent in short-term of $PM_{2.5}$-exposed mice. These outcomings in response to $PM_{2.5}$ seems to be mediated by sEV-induced crosstalk between lung and heart. The respiratory system derived sEV contains miR-421 and suppresses cardiac ACE2 expression, which causes cardiomyocytes apoptosis and cardiac dysfunction. Injection of GW4869 or DIZE can attenuate $PM_{2.5}$-induced cardiac dysfunction. Our study will help to understand the mechanism underlying ambient $PM_{2.5}$ and CVD development and provide potential new direction for therapeutical interventions for air pollution related disease therapy.

ACKNOWLEDGEMENTS

We thank Dr. Xi Hu (Quantum Design China & Delong Instruments) for supporting the TEM image acquisition of sEV in the present study. In addition, we appreciate the kindly help from Xiaoqi Hu on our experiment. This work was supported by the grants from National Key Research and Development Project (2018YFE0113500 to JJ Xiao), National Natural Science Foundation of China (82020108002, and 81911540486 to JJ Xiao, 82000253 to HY Wang, 81600008 to W Rui), the grant from Science and Technology Commission of Shanghai Municipality (20DZ2255400 and 21XD1421300 to JJ Xiao), the "Dawn" Program of Shanghai Education Commission (19SG34 to JJ Xiao), the Sailing Program from Science and Technology Commission of Shanghai (20YF1414000 to HY Wang), "Chenguang Program" of Shanghai Education Development Foundation and Shanghai Municipal Education Commission (20CG46 to HY Wang). JS is supported by Horizon2020 ERC-2016-COG EVICARE (725229).

CONFLICT OF INTEREST

The authors report no conflict of interest.

DATA AVAILABILITY STATEMENT

All data of the study are available from the corresponding author by request.

ORCID

Hongyun Wang https://orcid.org/0000-0003-2417-5924
Junjie Xiao https://orcid.org/0000-0002-9202-0003

REFERENCES

Abohashem, S., Osborne, M. T., Dar, T., Naddaf, N., Abbasi, T., Ghoneem, A., Radfar, A., Patrich, T., Oberfeld, B., Tung, B., Fayad, Z. A., Rajagopalan, S., & Tawakol, A. (2021). A leucopoietic-arterial axis underlying the link between ambient air pollution and cardiovascular disease in humans. *European Heart Journal*, *42*, 761–772. https://doi.org/10.1093/eurheartj/ehaa982

Arab, T., Mallick, E. R., Huang, Y., Dong, L., Liao, Z., Zhao, Z., Gololobova, O., Smith, B., Haughey, N. J., Pienta, K. J., Slusher, B. S., Tarwater, P. M., Tosar, J. P., Zivkovic, A. M., Vreeland, W. N., Paulaitis, M. E., & Witwer, K. W. (2021). Characterization of extracellular vesicles and synthetic nanoparticles with four orthogonal single-particle analysis platforms. *Journal of Extracellular Vesicles*, *10*, e12079. https://doi.org/10.1002/jev2.12079

Atkinson, R. W., Kang, S., Anderson, H. R., Mills, I. C., & Walton, H. A. (2014). Epidemiological time series studies of PM2.5 and daily mortality and hospital admissions: a systematic review and meta-analysis. *Thorax*, *69*, 660–665. https://doi.org/10.1136/thoraxjnl-2013-204492

Bai, L., Shin, S., Burnett, R. T., Kwong, J. C., Hystad, P., Van Donkelaar, A., Goldberg, M. S., Lavigne, E., Copes, R., Martin, R. V., Kopp, A., & Chen, H. (2019). Exposure to ambient air pollution and the incidence of congestive heart failure and acute myocardial infarction: A population-based study of 5.1 million Canadian adults living in Ontario. *Environment International*, *132*, 105004. https://doi.org/10.1016/j.envint.2019.105004

Barnes, P. J., Burney, P. G. J., Silverman, E. K., Celli, B. R., Vestbo, J., Wedzicha, J. A., & Wouters, E. F. M. (2015). Chronic obstructive pulmonary disease. *Nature Reviews Disease Primers*, *1*, 15076. https://doi.org/10.1038/nrdp.2015.76

Barr, R. G., Ahmed, F. S., Carr, J. J., Hoffman, E. A., Jiang, R., Kawut, S. M., & Watson, K. (2012). Subclinical atherosclerosis, airflow obstruction and emphysema: The MESA Lung Study. *European Respiratory Journal*, *39*, 846–854. https://doi.org/10.1183/09031936.00165410

Bei, Y., Xu, T., Lv, D., Yu, P., Xu, J., Che, L., Das, A., Tigges, J., Toxavidis, V., Ghiran, I., Shah, R., Li, Y., Zhang, Y., Das, S., & Xiao, J. (2017). Exercise-induced circulating extracellular vesicles protect against cardiac ischemia-reperfusion injury. *Basic Research in Cardiology*, *112*, 38. https://doi.org/10.1007/s00395-017-0628-z

Breitner, S., Schneider, A., Devlin, R. B., Ward-Caviness, C. K., Diaz-Sanchez, D., Neas, L. M., Cascio, W. E., Peters, A., Hauser, E. R., Shah, S. H., & Kraus, W. E. (2016). Associations among plasma metabolite levels and short-term exposure to PM2.5 and ozone in a cardiac catheterization cohort. *Environment International*, *97*, 76–84. https://doi.org/10.1016/j.envint.2016.10.012

Burrell, L. M., Risvanis, J., Kubota, E., Dean, R. G., Macdonald, P. S., Lu, S., Tikellis, C., Grant, S. L., Lew, R. A., Smith, A. I., Cooper, M. E., & Johnston, C. I. (2005). Myocardial infarction increases ACE2 expression in rat and humans. *European Heart Journal*, *26*, 369–375. discussion 322–364, https://doi.org/10.1093/eurheartj/ehi114

Cao, C., Jiang, W., Wang, B., Fang, J., Lang, J., Tian, G., Jiang, J., & Zhu, T. F. (2014). Inhalable microorganisms in Beijing's PM2.5 and PM10 pollutants during a severe smog event. *Environmental Science & Technology*, *48*, 1499–1507. https://doi.org/10.1021/es4048472

Chen, R., Qiao, L., Li, H., Zhao, Y., Zhang, Y., Xu, W., Wang, C., Wang, H., Zhao, Z., Xu, X., Hu, H., & Kan, H. (2015). Fine particulate matter constituents, nitric oxide synthase DNA methylation and exhaled nitric oxide. *Environmental Science & Technology*, *49*, 11859–11865. https://doi.org/10.1021/acs.est.5b02527

Chen, X., Guo, J., Huang, Y., Liu, S., Huang, Y., Zhang, Z., Zhang, F., Lu, Z., Li, F., Zheng, J. C., & Ding, W. (2020). Urban airborne PM2.5-activated microglia mediate neurotoxicity through glutaminase-containing extracellular vesicles in olfactory bulb. *Environmental Pollution*, *264*, 114716. https://doi.org/10.1016/j.envpol.2020.114716

Crackower, M. A., Sarao, R., Oudit, G. Y., Yagil, C., Kozieradzki, I., Scanga, S. E., Oliveira-Dos-Santos, A. J., Da Costa, J., Zhang, L., Pei, Y., Scholey, J., Ferrario, C. M., Manoukian, A. S., Chappell, M. C., Backx, P. H., Yagil, Y., & Penninger, J. M. (2002). Angiotensin-converting enzyme 2 is an essential regulator of heart function. *Nature*, *417*, 822–828. https://doi.org/10.1038/nature00786

Davel, A. P., Lemos, M., Pastro, L. M., Pedro, S. C., De André, P. A., Hebeda, C., Farsky, S. H., Saldiva, P. H., & Rossoni, L. V. (2012). Endothelial dysfunction in the pulmonary artery induced by concentrated fine particulate matter exposure is associated with local but not systemic inflammation. *Toxicology*, *295*, 39–46. https://doi.org/10.1016/j.tox.2012.02.004

Deng, X., Rui, W., Zhang, F., & Ding, W. (2013). PM2.5 induces Nrf2-mediated defense mechanisms against oxidative stress by activating PIK3/AKT signaling pathway in human lung alveolar epithelial A549 cells. *Cell Biology and Toxicology*, *29*, 143–157. https://doi.org/10.1007/s10565-013-9242-5

Dominici, F., Peng, R. D., Bell, M. L., Pham, L., Mcdermott, A., Zeger, S. L., & Samet, J. M. (2006). Fine particulate air pollution and hospital admission for cardiovascular and respiratory diseases. *Jama*, *295*, 1127–1134. https://doi.org/10.1001/jama.295.10.1127

Donoghue, M., Hsieh, F., Baronas, E., Godbout, K., Gosselin, M., Stagliano, N., Donovan, M., Woolf, B., Robison, K., Jeyaseelan, R., Breitbart, R. E., & Acton, S. (2000). A novel angiotensin-converting enzyme-related carboxypeptidase (ACE2) converts angiotensin I to angiotensin 1–9. *Circulation Research*, *87*, E1–9. https://doi.org/10.1161/01.res.87.5.e1

Evans, C. E., Miners, J. S., Piva, G., Willis, C. L., Heard, D. M., Kidd, E. J., Good, M. A., & Kehoe, P. G. (2020). ACE2 activation protects against cognitive decline and reduces amyloid pathology in the Tg2576 mouse model of Alzheimer's disease. *Acta Neuropathologica*, *139*, 485–502. https://doi.org/10.1007/s00401-019-02098-6

Femminò, S., Penna, C., Margarita, S., Comità, S., Brizzi, M. F., & Pagliaro, P. (2020). Extracellular vesicles and cardiovascular system: Biomarkers and cardio-protective effectors. *Vascular Pharmacology*, *135*, 106790. https://doi.org/10.1016/j.vph.2020.106790

Gangwar, R. S., Bevan, G. H., Palanivel, R., Das, L., & Rajagopalan, S. (2020). Oxidative stress pathways of air pollution mediated toxicity: Recent insights. *Redox Biology*, *34*, 101545. https://doi.org/10.1016/j.redox.2020.101545

Gao, J., Yuan, J., Wang, Q. ' e., Lei, T., Shen, X., Cui, B., Zhang, F., Ding, W., & Lu, Z. (2020). Metformin protects against PM2.5-induced lung injury and cardiac dysfunction independent of AMP-activated protein kinase alpha2. *Redox Biology*, *28*, 101345. https://doi.org/10.1016/j.redox.2019.101345

Greenfield, E. A. (2017). Sampling and preparation of mouse and rat serum. *Cold Spring Harbor Protocols*, *11*, pdb prot100271. https://doi.org/10.1101/pdb.prot100271

Guan, B., Wang, T.-L., & Shih, I.-M. (2011). ARID1A, a factor that promotes formation of SWI/SNF-mediated chromatin remodeling, is a tumor suppressor in gynecologic cancers. *Cancer Research*, *71*, 6718–6727. https://doi.org/10.1158/0008-5472.CAN-11-1562

Guillot, L., Nathan, N., Tabary, O., Thouvenin, G., Le Rouzic, P., Corvol, H., Amselem, S., & Clement, A. (2013). Alveolar epithelial cells: Master regulators of lung homeostasis. *International Journal of Biochemistry & Cell Biology*, *45*, 2568–2573. https://doi.org/10.1016/j.biocel.2013.08.009

Guo, H., lanYang, W., Jiang, L., Lyu, Y., Cheng, T., Gao, B., & Li, X. (2019). Association of short-term exposure to ambient air pollutants with exhaled nitric oxide in hospitalized patients with respiratory-system diseases. *Ecotoxicology and Environmental Safety*, *168*, 394–400. https://doi.org/10.1016/j.ecoenv.2018.10.094

Hayes, R. B., Lim, C., Zhang, Y., Cromar, K., Shao, Y., Reynolds, H. R., Silverman, D. T., Jones, R. R., Park, Y., Jerrett, M., Ahn, J., & Thurston, G. D. (2020). PM2.5 air pollution and cause-specific cardiovascular disease mortality. *International Journal of Epidemiology*, *49*, 25–35. https://doi.org/10.1093/ije/dyz114

He, M., Ichinose, T., Yoshida, S., Ito, T., He, C., Yoshida, Y., Arashidani, K., Takano, H., Sun, G., & Shibamoto, T. (2017). PM2.5-induced lung inflammation in mice: Differences of inflammatory response in macrophages and type II alveolar cells. *Journal of Applied Toxicology*, *37*, 1203–1218. https://doi.org/10.1002/jat.3482

Izzotti, A., Larghero, P., Longobardi, M., Cartiglia, C., Camoirano, A., Steele, V. E., & De Flora, S. (2011). Dose-responsiveness and persistence of microRNA expression alterations induced by cigarette smoke in mouse lung. *Mutation Research*, *717*, 9–16. https://doi.org/10.1016/j.mrfmmm.2010.12.008

Jacobs, D. R., Yatsuya, H., Hearst, M. O., Thyagarajan, B., Kalhan, R., Rosenberg, S., Smith, L. J., Barr, R. G., & Duprez, D. A. Jr. (2012). Rate of decline of forced vital capacity predicts future arterial hypertension: The Coronary Artery Risk Development in Young Adults Study. *Hypertension*, *59*, 219–225. https://doi.org/10.1161/HYPERTENSIONAHA.111.184101

Kalluri, R., & Lebleu, V. S. (2020). The biology, function, and biomedical applications of exosomes. *Science*, *367*(6478), eaau6977. https://doi.org/10.1126/science.aau6977

Kimura, T., Ferran, B., Tsukahara, Y., Shang, Q., Desai, S., Fedoce, A., Pimentel, D. R., Luptak, I., Adachi, T., Ido, Y., Matsui, R., & Bachschmid, M. M. (2019). Production of adeno-associated virus vectors for in vitro and in vivo applications. *Science Reports*, *9*, 13601. https://doi.org/10.1038/s41598-019-49624-w

Lambert, D. W., Lambert, L. A., Clarke, N. E., Hooper, N. M., Porter, K. E., & Turner, A. J. (2014). Angiotensin-converting enzyme 2 is subject to post-transcriptional regulation by miR-421. *Clinical Science (London, England: 1979)*, *127*, 243–249. https://doi.org/10.1042/CS20130420

Li, J., Hu, Y., Liu, L., Wang, Q., Zeng, J., & Chen, C. (2020). PM2.5 exposure perturbs lung microbiome and its metabolic profile in mice. *Science of the Total Environment*, *721*, 137432. https://doi.org/10.1016/j.scitotenv.2020.137432

Li, Q., Zhang, H., Jin, X., Cai, X., & Song, Y. (2021). Mechanism of haze pollution in summer and its difference with winter in the North China Plain. *Science of the Total Environment*, *806*, 150625. https://doi.org/10.1016/j.scitotenv.2021.150625

Liu, C., Chen, R., Sera, F., Vicedo-Cabrera, A. M., Guo, Y., Tong, S., Coelho, M., Saldiva, P. H. N., Lavigne, E., Matus, P., Valdes Ortega, N., Osorio Garcia, S., Pascal, M., Stafoggia, M., Scortichini, M., Hashizume, M., Honda, Y., Hurtado-Díaz, M., Cruz, J., … Kan, H. (2019). Ambient particulate air pollution and daily mortality in 652 cities. *New England Journal of Medicine*, *381*, 705–715. https://doi.org/10.1056/NEJMoa1817364

Liu, Y., Qian, X.-M., He, Q.-C., & Weng, J.-K. (2020). MiR-421 inhibition protects H9c2 cells against hypoxia/reoxygenation-induced oxidative stress and apoptosis by targeting Sirt3. *Perfusion*, *35*, 255–262. https://doi.org/10.1177/0267659119870725

Liu, Y., Wang, T., Si, B., Du, H., Liu, Y., Waqas, A., Huang, S., Zhao, G., Chen, S., & Xu, A. (2021). Intratracheally instillated diesel PM2.5 significantly altered the structure and composition of indigenous murine gut microbiota. *Ecotoxicology and Environmental Safety*, *210*, 111903. https://doi.org/10.1016/j.ecoenv.2021.111903

Ljungman, P. L. S., Li, W., Rice, M. B., Wilker, E. H., Schwartz, J., Gold, D. R., Koutrakis, P., Benjamin, E. J., Vasan, R. S., Mitchell, G. F., Hamburg, N. M., & Mittleman, M. A. (2018). Long- and short-term air pollution exposure and measures of arterial stiffness in the Framingham Heart Study. *Environment International*, *121*, 139–147. https://doi.org/10.1016/j.envint.2018.08.060

Long, M.-H., Zhu, X.-M., Wang, Q., Chen, Y., Gan, X.-D., Li, F., Fu, W.-L., Xing, W.-W., Xu, D.-Q., & Xu, D.-G. (2020). PM2.5 exposure induces vascular dysfunction via NO generated by iNOS in lung of ApoE-/- mouse. *International Journal of Biological Sciences*, *16*, 49–60. https://doi.org/10.7150/ijbs.36073

Madrigano, J., Baccarelli, A., Mittleman, M. A., Wright, R. O., Sparrow, D., Vokonas, P. S., Tarantini, L., & Schwartz, J. (2011). Prolonged exposure to particulate pollution, genes associated with glutathione pathways, and DNA methylation in a cohort of older men. *Environmental Health Perspectives*, *119*, 977–982. https://doi.org/10.1289/ehp.1002773

Madrigano, J., Kloog, I., Goldberg, R., Coull, B. A., Mittleman, M. A., & Schwartz, J. (2013). Long-term exposure to PM2.5 and incidence of acute myocardial infarction. *Environmental Health Perspectives*, *121*, 192–196. https://doi.org/10.1289/ehp.1205284

Manson, M. L., Säfholm, J., James, A., Johnsson, A.-K., Bergman, P., Al-Ameri, M., Orre, A.-C., Kärrman-Mårdh, C., Dahlén, S.-E., & Adner, M. (2020). IL-13 and IL-4, but not IL-5 nor IL-17A, induce hyperresponsiveness in isolated human small airways. *Journal of Allergy and Clinical Immunology*, *145*, 808–817.e802, https://doi.org/10.1016/j.jaci.2019.10.037

Newby, D. E., Mannucci, P. M., Tell, G. S., Baccarelli, A. A., Brook, R. D., Donaldson, K., Forastiere, F., Franchini, M., Franco, O. H., Graham, I., Hoek, G., Hoffmann, B., Hoylaerts, M. F., Künzli, N., Mills, N., Pekkanen, J., Peters, A., Piepoli, M. F., Rajagopalan, S., & Storey, R. F. (2015). Expert position paper on air pollution and cardiovascular disease. *European Heart Journal*, *36*, 83–93b. https://doi.org/10.1093/eurheartj/ehu458

Nishiyama, K., Morimoto, T., Furukawa, Y., Nakagawa, Y., Ehara, N., Taniguchi, R., Ozasa, N., Saito, N., Hoshino, K., Touma, M., Tamura, T., Haruna, Y., Shizuta, S., Doi, T., Fukushima, M., Kita, T., & Kimura, T. (2010). Chronic obstructive pulmonary disease – An independent risk factor for long-term cardiac and cardiovascular mortality in patients with ischemic heart disease. *International Journal of Cardiology*, *143*, 178–183. https://doi.org/10.1016/j.ijcard.2009.02.010

O'brien, K., Breyne, K., Ughetto, S., Laurent, L. C., & Breakefield, X. O. (2020). RNA delivery by extracellular vesicles in mammalian cells and its applications. *Nature Reviews Molecular Cell Biology*, *21*, 585–606. https://doi.org/10.1038/s41580-020-0251-y

Patel, V. B., Zhong, J. C., Grant, M. B., & Oudit, G. Y. (2016). Role of the ACE2/angiotensin 1–7 axis of the renin-angiotensin system in heart failure. *Circulation Research*, *118*, 1313–1326. https://doi.org/10.1161/CIRCRESAHA.116.307708

Pergoli, L., Cantone, L., Favero, C., Angelici, L., Iodice, S., Pinatel, E., Hoxha, M., Dioni, L., Letizia, M., Albetti, B., Tarantini, L., Rota, F., Bertazzi, P. A., Tirelli, A. S., Dolo, V., Cattaneo, A., Vigna, L., Battaglia, C., Carugno, M., … Bollati, V. (2017). Extracellular vesicle-packaged miRNA release after short-term exposure to particulate matter is associated with increased coagulation. *Particle and Fibre Toxicology*, *14*, 32. https://doi.org/10.1186/s12989-017-0214-4

Pope, C. A., Bhatnagar, A., Mccracken, J. P., Abplanalp, W., Conklin, D. J., & O'toole, T. 3rd (2016). Exposure to fine particulate air pollution is associated with endothelial injury and systemic inflammation. *Circulation Research*, *119*, 1204–1214. https://doi.org/10.1161/CIRCRESAHA.116.309279

Qiu, X., Wei, Y., Wang, Y., Di, Q., Sofer, T., Awad, Y. A., & Schwartz, J. (2020). Inverse probability weighted distributed lag effects of short-term exposure to PM2.5 and ozone on CVD hospitalizations in New England Medicare participants – Exploring the causal effects. *Environmental Research*, *182*, 109095. https://doi.org/10.1016/j.envres.2019.109095

Rodosthenous, R. S., Coull, B. A., Lu, Q., Vokonas, P. S., Schwartz, J. D., & Baccarelli, A. A. (2016). Ambient particulate matter and microRNAs in extracellular vesicles: A pilot study of older individuals. *Particle and Fibre Toxicology*, *13*, 13. https://doi.org/10.1186/s12989-016-0121-0

Shu, J., Chiang, K., Zempleni, J., & Cui, J. (2015). Computational characterization of exogenous MicroRNAs that can be transferred into human circulation. *Plos One*, *10*, e0140587. https://doi.org/10.1371/journal.pone.0140587

Sluijter, J. P. G., Davidson, S. M., Boulanger, C. M., Buzás, E. I., De Kleijn, D. P. V., Engel, F. B., Giricz, Z., Hausenloy, D. J., Kishore, R., Lecour, S., Leor, J., Madonna, R., Perrino, C., Prunier, F., Sahoo, S., Schiffelers, R. M., Schulz, R., Van Laake, L. W., Ytrehus, K., & Ferdinandy, P. (2018). Extracellular vesicles in diagnostics and therapy of the ischaemic heart: Position Paper from the Working Group on Cellular Biology of the Heart of the European Society of Cardiology. *Cardiovascular Research*, *114*, 19–34. https://doi.org/10.1093/cvr/cvx211

Spella, M., Lilis, I., & Stathopoulos, G. T. (2017). Shared epithelial pathways to lung repair and disease. *European Respiratory Review*, *26*, 170048. https://doi.org/10.1183/16000617.0048-2017

Stafoggia, M., Renzi, M., Forastiere, F., Ljungman, P., Davoli, M., De' Donato, F., Gariazzo, C., Michelozzi, P., Scortichini, M., Solimini, A., Viegi, G., Bellander, T., Ancona, C., Angelini, P., Argentini, S., Baldacci, S., Bisceglia, L., Bonafede, M., Bonomo, S., … Zengarini, N. (2020). Short-term effects of particulate matter on cardiovascular morbidity in Italy: a national analysis. *European Preventive Cardiology Journal*, zwaa084. https://doi.org/10.1093/eurjpc/zwaa084

Sun, B., Shi, Y., Li, Y., Jiang, J., Liang, S., Duan, J., & Sun, Z. (2020). Short-term PM2.5 exposure induces sustained pulmonary fibrosis development during post-exposure period in rats. *Journal of Hazardous Materials*, *385*, 121566. https://doi.org/10.1016/j.jhazmat.2019.121566

Van Eeden, S., Leipsic, J., Paul Man, S. F., & Sin, D. D. (2012). The relationship between lung inflammation and cardiovascular disease. *American Journal of Respiratory and Critical Care Medicine*, *186*, 11–16. https://doi.org/10.1164/rccm.201203-0455PP

Van Nunen, E., Hoek, G., Tsai, M.-Y., Probst-Hensch, N., Imboden, M., Jeong, A., Naccarati, A., Tarallo, S., Raffaele, D., Nieuwenhuijsen, M., Vlaanderen, J., Gulliver, J., Amaral, A. F. S., Vineis, P., & Vermeulen, R. (2021). Short-term personal and outdoor exposure to ultrafine and fine particulate air pollution in association with blood pressure and lung function in healthy adults. *Environmental Research*, *194*, 110579. https://doi.org/10.1016/j.envres.2020.110579

Wang, H., Guo, Y., Liu, L., Guan, L., Wang, T., Zhang, L., Wang, Y., Cao, J., Ding, W., Zhang, F., & Lu, Z. (2016). DDAH1 plays dual roles in PM2.5 induced cell death in A549 cells. *Biochimica Et Biophysica Acta*, *1860*, 2793–2801. https://doi.org/10.1016/j.bbagen.2016.03.022

Wang, H., Shen, X., Tian, G., Shi, X., Huang, W., Wu, Y., Sun, L., Peng, C., Liu, S., Huang, Y., Chen, X., Zhang, F., Chen, Y., Ding, W., & Lu, Z. (2018). AMPKalpha2 deficiency exacerbates long-term PM2.5 exposure-induced lung injury and cardiac dysfunction. *Free Radical Biology Medicine*, *121*, 202–214. https://doi.org/10.1016/j.freeradbiomed.2018.05.008

Wang, H., Shen, X., Tian, G., Shi, X., Huang, W., Wu, Y., Sun, L., Peng, C., Liu, S., Huang, Y., Chen, X., Zhang, F., Chen, Y., Ding, W., & Lu, Z. (2018). AMPKalpha2 deficiency exacerbates long-term PM2.5 exposure-induced lung injury and cardiac dysfunction. *Free Radical Biology & Medicine*, *121*, 202–214. https://doi.org/10.1016/j.freeradbiomed.2018.05.008

Wang, H., Xie, Y., Salvador, A. M., Zhang, Z., Chen, K., Li, G., & Xiao, J. (2020). Exosomes: Multifaceted messengers in atherosclerosis. *Current Atherosclerosis Reports*, *22*, 57. https://doi.org/10.1007/s11883-020-00871-7

Wang, K., Zhou, L.-Y., Wang, J.-X., Wang, Y., Sun, T., Zhao, B., Yang, Y.-J., An, T., Long, B., Li, N., Liu, C.-Y., Gong, Y., Gao, J.-N., Dong, Y.-H., Zhang, J., & Li, P.-F. (2015). E2F1-dependent miR-421 regulates mitochondrial fragmentation and myocardial infarction by targeting Pink1. *Nature Communication*, *6*, 7619. https://doi.org/10.1038/ncomms8619

Xu, F., Zhong, J.-Y., Lin, X., Shan, S.-K., Guo, B., Zheng, M.-H., Wang, Y., Li, F., Cui, R.-R., Wu, F., Zhou, E., Liao, X.-B., Liu, Y.-S., & Yuan, L.-Q. (2020). Melatonin alleviates vascular calcification and ageing through exosomal miR-204/miR-211 cluster in a paracrine manner. *Journal of Pineal Research*, *68*, e12631. https://doi.org/10.1111/jpi.12631

Xu, J., Zhang, W., Lu, Z., Zhang, F., & Ding, W. (2017). Airborne PM2.5-induced hepatic insulin resistance by Nrf2/JNK-mediated signaling pathway. *International Journal of Environmental Research and Public Health*, *14*, 787. https://doi.org/10.3390/ijerph14070787

Yue, W., Tong, L., Liu, X., Weng, X., Chen, X., Wang, D., Dudley, S. C., Weir, E. K., Ding, W., Lu, Z., Xu, Y., & Chen, Y. (2019). Short term Pm2.5 exposure caused a robust lung inflammation, vascular remodeling, and exacerbated transition from left ventricular failure to right ventricular hypertrophy. *Redox Biology*, *22*, 101161. https://doi.org/10.1016/j.redox.2019.101161

Zhang, Q., Zheng, Y., Tong, D., Shao, M., Wang, S., Zhang, Y., Xu, X., Wang, J., He, H., Liu, W., Ding, Y., Lei, Y., Li, J., Wang, Z., Zhang, X., Wang, Y., Cheng, J., Liu, Y., Shi, Q., … Hao, J. (2019). Drivers of improved PM2.5 air quality in China from 2013 to 2017. *PNAS*, *116*, 24463–24469. https://doi.org/10.1073/pnas.1907956116

Zhang, S., Breitner, S., Cascio, W. E., Devlin, R. B., Neas, L. M., Ward-Caviness, C., Diaz-Sanchez, D., Kraus, W. E., Hauser, E. R., Schwartz, J., Peters, A., & Schneider, A. (2021). Association between short-term exposure to ambient fine particulate matter and myocardial injury in the CATHGEN cohort. *Environmental Pollution*, *275*, 116663. https://doi.org/10.1016/j.envpol.2021.116663

Zhou, Q. L., Bai, Y. Z., Gao, J., Duan, Y., Lyu, Y. C., Guan, L. F., Elkin, K., Xie, Y. L., Jiao, Z., & Wang, H. Y. (2021). Human serum-derived extracellular vesicles protect A549 from PM 2.5-induced cell apoptosis. *Biomedical and Environmental Sciences*, *34*, 40–49. https://doi.org/10.3967/bes2021.006

SUPPORTING INFORMATION

Additional supporting information may be found in the online version of the article at the publisher's website.

How to cite this article: Wang, H., Wang, T., Rui, W., Xie, J., Xie, Y., Zhang, X., Guan, L., Li, G., Lei, Z., Schiffelers, R. M., Sluijter, J. P. G., & Xiao, J. (2022). Extracellular vesicles enclosed-miR-421 suppresses air pollution ($PM_{2.5}$)-induced cardiac dysfunction via ACE2 signaling. *Journal of Extracellular Vesicles*, *11,* e12222. https://doi.org/10.1002/jev2.12222